

# Study of galaxies in the Lynx-Cancer void. II. The element abundances

S. A. Pustilnik,<sup>1\*</sup> A. L. Tepliakova<sup>1\*</sup>, A. Y. Kniazev<sup>2</sup>

<sup>1</sup> *Special Astrophysical Observatory of RAS, Nizhnij Arkhyz, Karachai-Circassia 369167, Russia*

<sup>2</sup> *South African Astronomical Observatory, Cape Town, SAR*

Accepted March 25, 2011. Received February 21, 2011

## ABSTRACT

In the framework of the study of the evolutionary status of galaxies in the nearby Lynx-Cancer void, we present the results of the SAO RAS 6-m telescope spectroscopy for 20 objects in this region. The principal faint line [OIII] $\lambda$ 4363 Å, used to determine the electron temperature and oxygen abundance (O/H) by the classical method, is clearly detected in only about 2/3 of the studied objects. For the remaining galaxies this line is either faint or undetected. To obtain the oxygen abundances in these galaxies we as well apply the semi-empirical method by Izotov and Thuan, and/or the empirical methods of Pilyugin et al., which are only employing the intensities of sufficiently strong lines. We also present our O/H measurements for 22 Lynx-Cancer void galaxies, for which the suitable Sloan Digital Sky Survey (SDSS) spectra are available. In total, we present the combined O/H data for 48 Lynx-Cancer void galaxies, including the data adopted from the literature and our own earlier results. We make a comparison of their locations on the (O/H)– $M_B$  diagram with those of the dwarf galaxies of the Local Volume in the regions with denser environment. We infer that the majority of galaxies from this void on the average reveal an about 30% lower metallicity. In addition, a substantial fraction (not less than 10%) of the void dwarf galaxies have a much larger O/H deficiency (up to a factor of 5). Most of them belong to the tiny group of objects with the gas metallicity  $Z < Z_{\odot}/20$  or  $12 + \log(\text{O}/\text{H}) \lesssim 7.35$ . The surface density of very metal-poor galaxies ( $Z < Z_{\odot}/10$ ) in this region of the sky is 2–2.5 times higher than that, derived from the emission-line galaxy samples in the Hamburg-SAO and the SDSS surveys. We discuss possible implications of these results for the galaxy evolution models.

**Key words:** galaxies: dwarf – galaxies: evolution – galaxies: abundances: – large-scale structure of Universe

## 1 INTRODUCTION

The relation between the properties of galaxies and their environment is studied and discussed for quite a long time. Many aspects of the accelerated galaxy evolution in the dense environment (galaxy clusters and compact groups) are discovered and explained. On the opposite edge of the galaxy density range, for the most rarefied environment (or voids), a certain advance was made in the study of galaxy properties, namely, their colour, the rates of star formation, etc. mainly due to the huge data supply by the Sloan Digital Sky Survey (SDSS) Abazajian et al. (2009) (see Pustilnik and Tepliakova (2011) for details and references).

However, these studies did not deal directly with the evolutionary status of the void galaxies. Since the effect of environment is expected to be the largest for the galaxies of the smallest masses, it is reasonable to study the galaxies in the nearby voids to trace any possible differences in the evolution of dwarf galaxies. There one can make a sample of the least massive and luminous objects. In Paper I Pustilnik and Tepliakova (2011) we described a sample of 79 galaxies in one of the nearest voids, the Lynx-Cancer void, with total size in excess of 16 Mpc, and centre located 18 Mpc away. The sample consists mainly of dwarf disc (irregular and late-type spiral) galaxies. About a half of them belong to the Low Surface Brightness (LSB) galaxies. This means that the central surface brightness of the underlying disc of these objects, corrected for extinction and disc inclination amounts to  $\mu_{0,B,i,c} > 23^m/\square''$ . The absolute mag-

\* sap@sao.ru (SAP), arina@sao.ru (ALT), akniazev@sao.ac.za (AYK)

nitude  $M_B$  of the sample galaxies lies between  $-11.9$  and  $-18.4$ , with the median value of about  $-14.5$ . According to the preliminary estimates the sample is nearly complete for the luminosities of  $-14 > M_B$ .

The main goal of Paper I was to form a sufficiently deep and large sample of galaxies in the individual void in order to study their evolutionary parameters and spatial distribution. The evolutionary status is characterized by the sufficiently easily assessed parameters: the gas metallicity (in our case, the oxygen abundance (O/H) in the regions of the current star formation (SF)) and the mass fraction of gas. The latter parameter is measured from the direct measurements of the gas mass via HI 21 cm line flux (corrected for the fraction of helium) and from the model-dependent stellar mass  $M_*$ . The latter is determined from the optical luminosity and the ratio  $M_*/L(\text{opt})$ , which depends on the galaxy colours. One more parameter related to the galaxy evolution is the age of the oldest population visible in the well-resolved galaxy images. It is usually assumed that the old stellar population is the most representative in the outer parts of galaxies, outside the current SF regions. The latter mainly reside near the galaxy centres or within the ‘optical’ radius of the galaxy disc. In most of galaxies, the population of the outer regions reveals colours typical of stars aged  $T \gtrsim 10$  Gyr. Only in several galaxies with a very low metallicity (I Zw 18 and similar) this old population has not been detected (Guseva et al. (2003)). Lately, several galaxies with younger populations, i.e. with  $T_{\text{old}} \lesssim (1-3)$  Gyr have been discovered namely in the voids Pustilnik et al. (2003a, 2004b); Pustilnik, Kniazev & Pramskij (2005); Pustilnik et al. (2008, 2010).

Within the ongoing project on the study of the evolutionary status of the Lynx-Cancer void galaxies, we undertook the spectral survey of part of our sample with the 6-m BTA telescope of the Special Astrophysical Observatory of Russian Academy of Sciences (SAO RAS) with the goal to obtain the O/H of their gas. For a part of the sample, we also used the SDSS spectra. For a comparative analysis of the O/H parameter in the void galaxies with those in a denser environment, we also included several O/H estimates for the void galaxies published in the literature.

The amount of evidence for the existence of void galaxies, representing a less evolved population was growing during the last decade Peebles (2001); Pustilnik et al. (2003a, 2004a); Pustilnik, Kniazev & Pramskij (2005); Pustilnik et al. (2006). However, this data concerned mainly the galaxies with active star formation due to selection effects. Therefore, we need to address this issue using a more general approach, which is mainly aimed on the analysis of more or less typical late-type galaxies. As noted before, the less luminous and massive the galaxy, the more it is susceptible to external perturbations. Therefore, to study probable effects of the global environment, one needs a sample of relatively nearby galaxies.

The lay-out of the paper is as follows. Section 2 describes the spectral observations and primary reduction of the BTA data, the spectral data from the SDSS database and their analysis, as well as the further analysis of emission-line spectra. Section 3 presents the description of the obtained results, the tables of measured line intensities and derived physical parameters and element abundances. In Section 4 we discuss all the results on the O/H for the Lynx-

Cancer void galaxy sample accumulated so far, and compare them with O/H values for the galaxies residing in denser regions. The summary of our main results is given in Section 5. Appendix A contains plots with the spectra of all objects, obtained at the BTA or taken from the SDSS database. Appendix B presents the tables with relative line intensities, as well as the derived O/H for all galaxies.

## 2 OBSERVATIONS AND REDUCTION

The observations presented in the paper were conducted at the BTA in the period between 2002 and 2009 (see the journal of observations in Table 1). Apart from the galaxies residing in the Lynx-Cancer void, we also observed as back-up targets eight galaxies which populate the adjacent denser regions. They are presented in the bottom of the same Table below the solid line. The galaxy UGC 731 is the object residing in the nearby Cepheus void.

The majority of observations were conducted with the multimode SCORPIO instrument (Afanasiev & Moiseev 2005), installed at the prime focus of the BTA between January 12, 2007 and February 19, 2009. The grism VPHG550G and the 2K×2K EEV 42-40 CCD detector were used for all observations except the nights of January 21 and 22, 2009, when the 2K×4K EEV 42-90 CCD detector was used. For several earlier observations we used the UAGS spectrograph, installed in the prime focus of BTA, with the grating 400 grooves  $\text{mm}^{-1}$  and 1K×1K pixel Photometrics-1024 CCD detector (Afanasiev et al. 1995). The respective spectral ranges, spectral resolution, exposure times and seeings for each object are presented in Table 1. The scale along the slit (after binning) was  $0''.36 \text{ pixel}^{-1}$  in all observations with the SCORPIO and  $0''.40 \text{ pixel}^{-1}$  in the observations with the UAGS. The object spectra were complemented by the reference spectra of a He-Ne-Ar lamp for the wavelength calibration. The spectral standard stars Feige 34, BD+28°4211, G191B2B and others from the list of Bohlin (1996) were observed for the flux calibration several times per night. The slit was positioned on H II regions either found in the literature (van Zee 1997; Karachentsev & Kaisin 2010) or identified in the images of the studied galaxies, obtained with the SCORPIO with the medium-width filter SED665 (FWHM=191 Å, centred at  $\lambda 6622$  Å).

For 22 Lynx-Cancer void galaxies (4 of them are from the BTA program) we derived useful element abundance estimates from the spectra in the SDSS DR7 database. The SDSS spectra were obtained through a  $3''$  round aperture with the multi-object fiber spectrograph, and processed with the SDSS standard pipeline. A more detailed description can be found in (Gunn et al. 1998; Abazajian et al. 2009).

All spectral data reduction (for BTA observations) was performed using the technique, similar to that, described in Pustilnik, Kniazev & Pramskij (2005). The standard pipeline of long-slit spectra reduction uses the IRAF<sup>1</sup>

<sup>1</sup> IRAF: the Image Reduction and Analysis Facility is distributed by the National Optical Astronomy Observatory, which is operated by the Association of Universities for Research in Astronomy, Inc. (AURA) under cooperative agreement with the National Science Foundation (NSF).

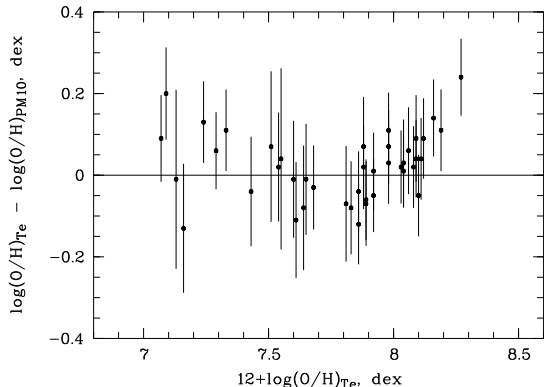


**Figure 1.** The illustration of the general consistency of O/H values derived via the method of Pilyugin and Mattsson (PM10) with those derived by the classic  $T_e$  method. Out of 42 galaxies, shown in the plot, 28 are the subsample of the nearby non-BCG galaxies from the SHOC catalog. The data for 14 galaxies with  $12+\log(\text{O}/\text{H}) < 7.65$ , which are very few in the SHOC, are adopted from other sources Kniazev et al. (2003); Izotov & Thuan (2007); van Zee (2000); Pustilnik, Kniazev & Pramskij (2005).

and MIDAS<sup>2</sup> codes. It implies the following steps: the removal of cosmic ray hits, bias subtraction, flat-field correction, wavelength calibration, night-sky background subtraction. Then, using the data on the spectrophotometry of standard stars, we obtained the curves of spectral sensitivity in a given night, and all spectra were transformed to the absolute fluxes. Finally, individual 1D spectra of the target HII-regions were extracted by the summation of several rows (typically 5–10, where the faint line [O III]  $\lambda 4363$ , necessary to make the temperature estimate  $T_e$  is visible). The emission line intensities with their errors were measured in the individual 1D spectra using the method, described in detail in Kniazev et al. (2004). Finally, the element abundances were calculated using the procedures described in Kniazev et al. (2008) and references therein.

### 3 RESULTS

The synopsis of the results of O/H measurements is laid out in Table 2 and Figures 2,3 and discussed in Section 4. Below, we overview the obtained results in more detail.

Figures A.1 and A.2 in Appendix A present the mosaic of 20 spectra of 20 Lynx-Cancer void galaxies, observed at the BTA. Tables B.1–B.7 in Appendix B list measured relative line intensities of all relevant emission lines and their fluxes corrected for extinction and the underlying Balmer-line absorptions. This procedure is performed iteratively by the technique, described by Izotov et al. (1994). All the flux measurements follow the method described by Kniazev et al. (2004). The measured line flux values in the H $\beta$  line are given in the units of  $10^{-16}$  erg s $^{-1}$  cm $^{-2}$ . Figure A.5 in Appendix A presents the BTA spectra of 10 HII regions in 9 galaxies residing outside the Lynx-Cancer void.

The relative emission line fluxes for these galaxies, corrected for extinction and the underlying Balmer-line absorptions are presented in Tables 19.B–22.B of Appendix B. Here under the name of each galaxy we indicated the coordinates of the HII region, for which the analyzed spectrum is obtained. Figures A.3 and A.4 of Appendix A present the mosaic of spectra of 20 Lynx-Cancer void galaxies, extracted from the SDSS DR7 database. In Tables 8.B–14.B of Appendix B we present for the SDSS spectra the measured relative line intensities of all relevant emission lines, and their fluxes corrected for extinction and the underlying Balmer-line absorptions, similar to those presented above for the BTA spectra. The flux of the [OII] $\lambda 3737$  line is shown in parentheses, since this is not the measured value, but the one recalculated from the line flux of the [OII] $\lambda 7320, 7330$  lines, as described below.

Tables B.15 and B.16 in Appendix B present the electron temperatures (based on the BTA spectra) we measured in the emission zones of the OIII and OII ions and their abundances along with the total O/H abundance, derived for the line fluxes with the classic  $T_e$ -method, according to the scheme described in Kniazev et al. (2008). For the cases when the [OIII] $\lambda 4363$  line is faint or undetectable, we also apply the semi-empirical method of Izotov and Thuan Izotov & Thuan (2007) (based on the  $T_e$  estimate, derived from the fluxes of the [OII] $\lambda 3727$  and [OII] $\lambda 4959, 5007$  lines), which gives the O/H well consistent with that derived by the classical  $T_e$ -method for the range of  $12+\log(\text{O}/\text{H}) \lesssim 7.9$ . However, according to our tests, the semi-empirical method for the range of  $12+\log(\text{O}/\text{H}) \gtrsim 7.9$ , gives a systematically lower O/H, with the difference of  $\Delta(\text{O}/\text{H}) \sim 0.10$  dex for the O/H, derived with the  $T_e$ -method in the range of  $12+\log(\text{O}/\text{H}) = 7.9 - 8.1$ . Therefore, when we used the semi-empirical method for the above O/H range (as indicated, e.g., by other methods), the respective correction was applied. We also show the O/H values derived via the empirical methods from Pilyugin and Mattsson (hereinafter referred to as PM10) Pilyugin and Mattsson (2011), and Pilyugin et al. (hereinafter referred to as PVT10) Pilyugin et al. (2010) for the cases when they have relatively small errors. Similar data for the non-void BTA observations are presented in Table B.23.

Tables B.17–B.18 of Appendix B present similar parameters for the void galaxies, derived from the SDSS DR7 data. Since for the galaxies with redshifts  $z \lesssim 0.025$  the line [OII] $\lambda 3727$  is out of the range covered by the SDSS spectra, one can use the flux in the [OII] $\lambda 7320, 7330$  lines to determine the O/H via the classical method Kniazev et al. (2003, 2004). For the cases when the [OIII] $\lambda 4363$  line is faint or undetectable, the semi-empirical method can be applied. In this case the line intensities of [OII] $\lambda 7320, 7330$  can be transformed into the line intensity of [OII] $\lambda 3727$  through the dependence between these parameters, presented in the graphic form by Aller Aller (1984). For the low electron density ( $N_e \lesssim 10^2$ ) the ratio of intensities of the [OII] $\lambda 3727$  lines and the sum of intensities of the [OII] $\lambda 7320, 7330$  lines, or the “O-ratio” as a function of  $t$  for  $1 < t < 2$  ( $t = T_e/10000$ ) is well approximated by the formula:

$$\log(\text{O} - \text{ratio}) = 1.77 - 2.06 \times \log(t) + 2.318 \times \log(t)^2.$$

The fluxes in the OII $\lambda 3727$  line, listed in Tables B.8–B.13 of Appendix B for the SDSS spectra are extrapolated from fluxes in the [OII] $\lambda 7320, 7330$  lines at the temperature  $T_e$ , adopted from a few iterations. This is why they should be treated as approximate estimates.

<sup>2</sup> MIDAS is an acronym for the European Southern Observatory package – Munich Image Data Analysis System.

**Table 1.** Journal of the 6 m telescope spectral observations

Name	Date	Exp. time [s]	Wavelength Range [Å]	Disp. [Å/px]	Spec. res.(Å)	Seeing [ʹ]	Air mass	Grism or grating	Detector
(1)	(2)	(3)	(4)	(5)	(6)	(7)	(8)	(9)	(10)
UGC 3475	2008.01.12	3×900	3500 – 7500	2.1	12.0	1.2	1.08	VPHG550G	2K×2K
UGC 3476	2007.12.16	4×900	3500 – 7500	2.1	12.0	2.5	1.03	VPHG550G	2K×2K
UGC 3501	2008.11.26	4×900	3500 – 7500	2.1	12.0	1.4	1.13	VPHG550G	2K×2K
UGC 3600	2008.11.26	3×900	3500 – 7500	2.1	12.0	1.4	1.19	VPHG550G	2K×2K
UGC 3672	2003.12.24	2×900	3500 – 7500	2.1	12.0	1.2	1.02	G400	1K×1K
UGC 3698	2008.11.26	3×900	3500 – 7500	2.1	12.0	1.7	1.05	VPHG550G	2K×2K
NGC 2337	2008.12.18	3×420	3500 – 7500	2.1	12.0	2.0	1.09	VPHG550G	2K×2K
UGC 3817	2008.01.12	3×900	3500 – 7500	2.1	12.0	1.2	1.03	VPHG550G	2K×2K
UGC 3860	2008.12.18	3×600	3500 – 7500	2.1	12.0	2.0	1.10	VPHG550G	2K×2K
UGC 3876	2009.01.22	4×900	3500 – 7500	2.1	12.0	1.5	1.09	VPHG550G	2K×4K
UGC 4117	2002.01.13	2×900	3500 – 7500	2.1	11.0	1.7	1.13	G400	1K×1K
MCG7-17-19	2003.01.02	1×1200	3500 – 7500	2.1	11.0	2.5	1.30	G400	1K×1K
KUG 0821+321	2009.02.19	3×900	3500 – 7500	2.1	12.0	1.8	1.03	VPHG550G	2K×2K
SDSS J0843+4025	2007.01.12	3×900	3500 – 7500	2.1	12.0	2.5	1.39	VPHG550G	2K×2K
UGC 4704	2009.01.22	2×900	3500 – 7500	2.1	12.0	1.5	1.32	VPHG550G	2K×4K
UGC 5272B	2008.01.12	4×900	3500 – 7500	2.1	12.0	1.0	1.12	VPHG550G	2K×2K
UGC 5272	2002.01.12	1×1200	3500 – 7500	2.1	11.0	1.6	1.04	G400	1K×1K
SDSS J1000+3032	2009.01.21	3×900	3500 – 7500	2.1	12.0	1.4	1.39	VPHG550G	2K×4K
UGC 5427	2007.01.12	5×900	3500 – 7500	2.1	12.0	2.4	1.07	VPHG550G	2K×2K
UGC 5464	2008.01.12	3×900	3500 – 7500	2.1	12.0	1.0	1.29	VPHG550G	2K×2K
UGC 731	2008.11.26	4×900	3500 – 7500	2.1	12.0	1.5	1.02	VPHG550G	2K×2K
SDSS J0839+3140	2009.01.22	2×900	3500 – 7500	2.1	12.0	1.5	1.18	VPHG550G	2K×4K
UGC 4787	2009.01.22	4×900	3500 – 7500	2.1	12.0	1.9	1.06	VPHG550G	2K×4K
KUG 1004+392	2008.12.18	3×600	3500 – 7500	2.1	12.0	1.5	1.02	VPHG550G	2K×2K
UGC 5451	2008.01.13	3×900	3500 – 7500	2.1	12.0	1.2	1.05	VPHG550G	2K×2K
SDSS J1031+2801	2009.02.19	3×900	3500 – 7500	2.1	12.0	1.7	1.29	VPHG550G	2K×2K
NGC 3274	2009.02.19	2×900	3500 – 7500	2.1	12.0	1.7	1.60	VPHG550G	2K×2K
UGC 5764	2009.01.22	3×900	3500 – 7500	2.1	12.0	2.0	1.22	VPHG550G	2K×4K
UGC 6055	2009.02.19	2×900	3500 – 7500	2.1	12.0	1.7	1.41	VPHG550G	2K×2K

Apart from that, we used the empirical method for estimating the O/H, recently proposed by Pilyugin and Mattsson (PM10) Pilyugin and Mattsson (2011), which exploits both the fluxes of strong lines [OIII]λ4959, 5007 and the fluxes of the [NII]λ6548, 6584 and [SII]λ6716, 6730 lines. To check how well the method of Pilyugin and Mattsson Pilyugin and Mattsson (2011) approximates the real O/H values in the studied galaxies, we made a comparison of O/H( $T_e$ ) values, known with the accuracy of  $\sigma_{O/H} \lesssim 0.06$  with the O/H values derived via the formulae from Pilyugin and Mattsson (2011). To this end, we used 14 different measurements for the galaxies with  $12+\log(O/H) \lesssim 7.65$  from the papers Kniazev et al. (2003); Izotov & Thuan (2007); van Zee (2000); Pustilnik, Kniazev & Pramskij (2005) and 28 galaxies with the best O/H measurements from the subsample of nearby non-BCG galaxies from the SHOC catalog Kniazev et al. (2004), based on the SDSS spectra. Figure 1 illustrates the difference  $\Delta \log(O/H) = \log(O/H(\text{PM10})) - \log(O/H(T_e))$  versus O/H( $T_e$ ) for these galaxies. In the range of  $12+\log(O/H)$  between 7.1 and 8.3, which fully covers the range of O/H for our void sample, there is no systematic shift between these two methods. The scatter around the zero line corresponds

to the estimated root mean square errors of both O/H values.

## 4 DISCUSSION

Table 2 summarizes the information on the Lynx-Cancer void galaxies with the currently available O/H data, which can be used for the subsequent statistical analysis. The following information is presented. Column 1 gives the galaxy name, 2 and 3—right ascension and declination (J2000); columns 4 and 5 list the J2000 coordinates of the HII region, for which the spectrum was obtained; column 6 gives the heliocentric velocity (in km s<sup>-1</sup>); column 7—the distance in Mpc relative to the Local Group centre. Columns 8 and 9 present the adopted total  $B$ -magnitude and the respective absolute magnitude. All these parameters (except for the coordinates of the HII region) are taken from Table 2 of Paper I. In cases when the O/H was adopted from literature, we do not list the region coordinates and refer the reader to the original paper. In Column 10 we present the value of O/H adopted for the further analysis. It can come from different sources, indicated in Column 11 as follows: (1) the weighted mean O/H for two or more HII regions in the same galaxy from the BTA data, evaluated

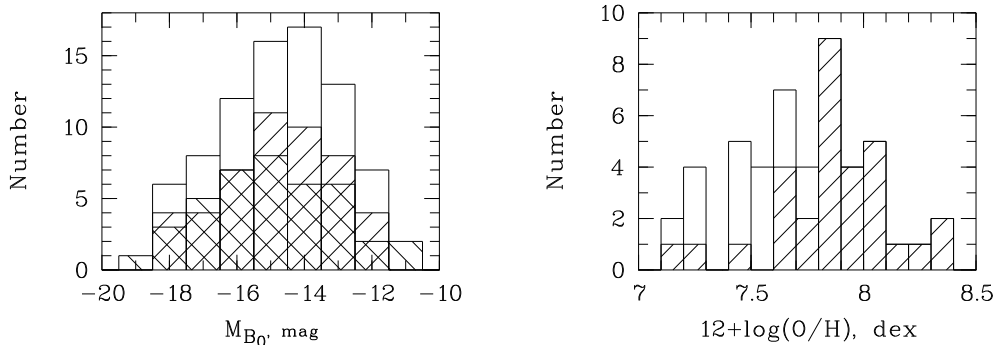


**Figure 2.** **Left panel:** the distribution of absolute magnitudes  $M_{B,0}$  for 48 galaxies with known O/H (hatched) relative to the same distribution for all 79 Lynx-Cancer void galaxies. For a comparison, the inverse hatching shows the distribution of  $M_{B,0}$  for 40 low-mass late-type galaxies from van Zee & Haynes (2006). **Right panel:** the distribution of all O/H values available to date for 48 galaxies Lynx-Cancer void galaxies and for their subsample of 31 objects with  $M_B < -14.0$  (hatched), i.e. for the luminosity range, in which the void sample is expected to be almost complete.

with the classical  $T_e$ -method; (2) the most probable O/H estimate from the BTA spectra, based on the combination of results of the classical  $T_e$ -method, the semi-empirical method Izotov & Thuan (2007) and the empirical methods from Pilyugin and Mattsson (2011); Pilyugin et al. (2010); (3) the same as in (2), but based on the SDSS spectra; (4) O/H, adopted from the literature and rescaled to the new scale Izotov et al. (2006) (if necessary).

The left plot of Fig. 2 presents the distributions of 48 Lynx-Cancer void galaxies with known O/H (the hatched histogram) compared to the statistics of the full void sample of 79 galaxies, which demonstrates the galaxy fractions with known O/H in each luminosity bin. For a comparison, the histogram with the inverse hatching<sup>3</sup> and in a wider range shows a similar distribution for 40 sample galaxies from van Zee & Haynes (2006), used to check the effect of the neighbourhood (see below). The void galaxies with known O/H are distributed more or less homogeneously over the whole luminosity range, with the average fraction of about 0.6. This allows to conclude that the real O/H distribution of the void galaxies does not differ significantly from that shown in the right panel for 48 galaxies with known O/H. In this panel the hatched histogram demonstrates the O/H distribution for 31 galaxies with  $M_B < -14.0$ , i.e. for the range, where the void galaxy sample is expected to be almost complete. Therefore, the tail of distribution with very metal-poor galaxies ( $7.1 < 12 + \log(O/H) < 7.5$ ) should be treated as a trustworthy.

#### 4.1 L–Z relationship for void galaxies

To examine how much the metallicities of the Lynx-Cancer void galaxies differ from those of the galaxies, residing in denser environments, one can use the empirical relationships between the O/H and  $M_B$  for the dwarf galaxy samples in the Local Volume and its surroundings (van Zee & Haynes 2006). However, we need to eliminate the systematic differences in the O/H scale, i.e. to account for small changes in

the O/H scale used in recent papers (including the O/H values, presented here) with respect to the scale used in earlier papers, on which the “standard” relationship O/H– $M_B$  we further use is based. This O/H scale variation, suggested by Izotov et al. (2006), is related to the changes in the atomic constants, used in the calculations. When the respective correction is made, the original formula for the L–Z relationship from van Zee & Haynes (2006)

$$12 + \log(O/H) = 5.65 - 0.149 \cdot M_B$$

transforms to

$$12 + \log(O/H) = 5.60 - 0.154 \cdot M_B$$

This relationship is illustrated in Fig. 3 by a straight solid line.

This figure also demonstrates similar relationships derived for different samples of late-type galaxies within the Local Volume. The dashed line, running a bit higher than the solid line describes the relationship for the sample from van Zee et al. (2006). The dotted line, running almost along the solid line shows a similar relationship derived by Lee et al. Lee et al. (2003) for the late-type dwarf galaxies from the nearby groups within the radius of 5 Mpc. Since all the three lines are very close to each other, they probably describe the same general relationship. For the further comparison with the “standard” relationship we adopt the one, derived in van Zee & Haynes (2006), since it has the smallest scatter,  $\sigma(O/H) \sim 0.15$  dex. To demonstrate a significant deviation of void galaxies from the “standard” relationship, we also plotted in Fig. 3 the dash-dotted lines, running 0.15 dex lower and higher than the solid “standard” line from van Zee & Haynes (2006).

The analysis of the O/H values of void galaxy in the L–Z diagram shows a clear systematic shift to the lower median values relative to the ‘standard’ line for every bin of the  $M_B$  range. Even if we exclude from the consideration six objects with the lowest O/H (i.e. with  $12 + \log(O/H) \lesssim 7.35$ ) as probably having atypical evolution histories or relatively small ages, the remaining galaxies will be mostly distributed below the ‘standard’ line. Their distribution becomes more symmetrical relative to the line parallel to the ‘standard’ L–Z line, shifted down by about 0.12 dex. This implies that about 85–90% quite typical galaxies, populating this void

<sup>3</sup> Right hatching—from the bottom left corner to the top right corner, the inverse hatching is perpendicular to it.

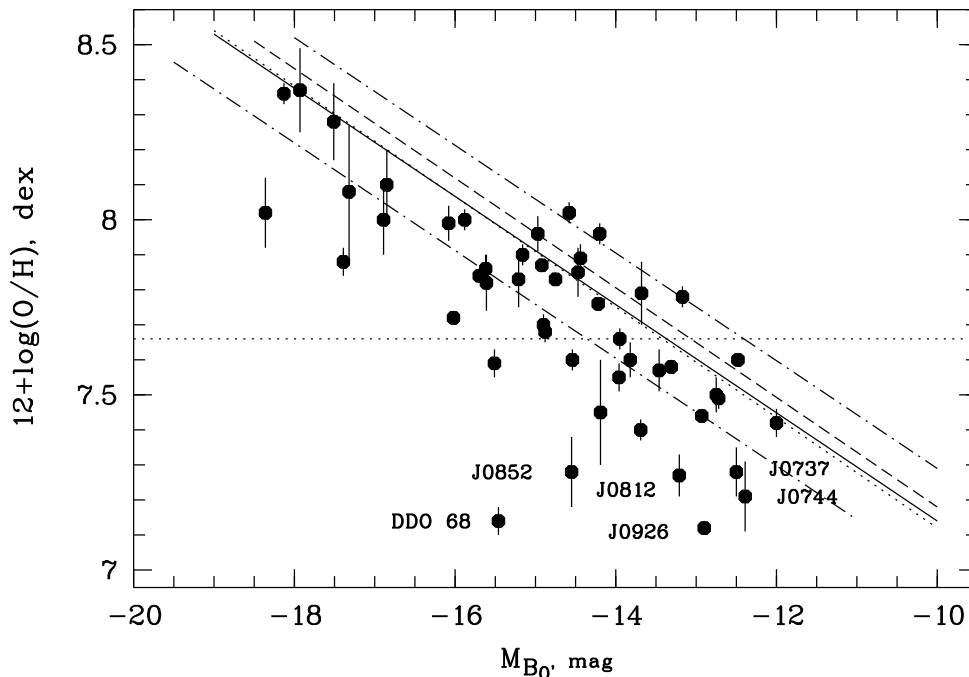


**Figure 3.** The Luminosity-Metallicity (L-Z) relationship for 48 Lynx-Cancer void galaxies. The solid, dashed and dotted lines mark the known linear fits for the L-Z relationship, obtained for 3 samples: isolated late-type galaxies van Zee & Haynes (2006), nearby dI galaxies van Zee et al. (2006), and nearby dI and I galaxies from Lee et al. Lee et al. (2003). Two dashed-dotted lines are drawn 0.15 dex lower and higher than the solid line, for which the (computed in van Zee & Haynes (2006)) root mean squared deviation is 0.15 dex. If the O/H galaxy distribution in this void corresponded to that, for which the “standard” L-Z relationship was obtained, one would expect that about 1/6 of galaxies out of the total of 48 galaxies (i.e. 8 objects) would appear below the bottom dashed-dotted line. In the reality though, 20 void galaxies made it into this region.

show a sizable deficiency of oxygen (on the average not less than 30%) relative to the galaxies used in constructing the ‘standard’ L-Z relation in the Local Volume. An alternative interpretation of the observed shift as a luminosity increase at the same metallicity seems unlikely. Indeed, an average shift by about 0.12 dex at a fixed  $M_B$  corresponds to a shift of 0.75 mag in  $M_B$  at the fixed O/H value, i.e. to the brightening by a factor of 2. This is a typical value for BCG-type galaxies (see, e.g., Papaderos et al. (2008)). However, in the discussed sample of void galaxies only two galaxies belong to this type: HS 0822+3542 and HS 1013+3809. The position of the former can be explained by a shift with respect to the “standard” line (via brightening) by about 1 magnitude. However, for the latter we would have to assume a brightening by about 2.5 magnitudes. The rest of the galaxies, as described in Paper I, belong to the late spirals and irregulars, in which the luminosities of the brightest HII regions are small compared to the total luminosity of the galaxy.

A large scatter of actively star-forming galaxies in the L-Z diagram, especially in the region of very low metallicities ( $12+\log(\text{O}/\text{H}) < 7.65$ ), was already noted in the literature (e.g., Kniazev et al. 2003; Guseva et al. 2009). For such galaxies, several possible evolutionary scenarios were suggested. One of them implies the genuine non-evolved galaxies. It is likely that namely in the void environments with low density of the surrounding galaxies, such “young” very metal-poor galaxies could greatly contribute to the general

galaxy population and hence lead to the greater scatter of the galaxy localisation in L-Z diagram.

#### 4.2 The most metal-poor Lynx-Cancer void galaxies

Coming back to the subject of the most metal-deficient and unusual dwarf galaxies, let us discuss them in more detail. These include a Blue Compact Galaxy HS 0822+3542 with the lowest metallicity ( $12+\log(\text{O}/\text{H})=7.44$ ) among all the BCG galaxies of the Local Volume and its surroundings, and its companion, a very blue (and presumably relatively young) galaxy of low surface brightness (LSBD) SAO 0822+3545 (Pustilnik et al. 2003a, and a paper in preparation). Other representatives of this void galaxy population are DDO 68 and SDSS J0926+3343 with  $12+\log(\text{O}/\text{H})$ , amounting to 7.14 and 7.12, respectively. These are the most metal-poor galaxies known after SBS 0335-052W and SDSS J0015+0104 (Izotov et al. 2009; Guseva et al. 2009). Situated on the mutual distance of only 1.6 Mpc, both of them are also unusual by the blue colours of their outer parts, indicating the ages of the oldest visible stellar population of  $\lesssim 1-3$  Gyr (Pustilnik et al. 2008, 2010), what is in drastic contrast with the situation in the absolute majority of other dwarf galaxies known to date.

In addition to these galaxies, the following void objects are among the most metal-poor: SDSS J0812+4836, with  $\text{O}/\text{H}=7.27$  dex (Izotov & Thuan 2007), two LSBD

**Table 2.** Main galaxy parameters in the Lynx-Cancer void with the known O/H values

No.	Name or prefix (1)	Coordinates (J2000) of galaxy		Coordinates (J2000) of HII region		$V_{\text{hel}}$ , km/s (6)	D, Mpc (7)	$B_{\text{tot}}$ , mag (8)	$M_{\text{B}}^{\dagger}$ , mag (9)	12+log(O/H) adopt. (10)	Source O/H (11)
		(2)	(3)	(4)	(5)						
1	UGC3475	06 30 28.86	+39 30 13.6	06 30 27.02	+39 30 26.3	487	10.30	14.97	-15.88	8.00±0.03	2
2	UGC3476	06 30 29.22	+33 18 07.2	06 30 29.27	+33 18 05.0	469	9.84	14.96	-16.02	7.72±0.02	2
3	UGC3501	06 38 38.40	+49 15 30.0	06 38 40.24	+49 15 28.6	449	10.07	17.20	-13.31	7.58±0.02	2
4	UGC3600	06 55 40.00	+39 05 42.8	06 55 41.90	+39 06 21.7	412	9.30	16.18	-13.95	7.66±0.03	2
5	UGC3672	07 06 27.56	+30 19 19.4	07 06 25.46	+30 19 36.4	994	16.93	15.40	-16.08	7.99±0.05	2
6	UGC3698	07 09 16.80	+44 22 48.0	07 09 18.15	+44 22 43.7	422	9.60	15.41	-14.92	7.87±0.02	2
7	NGC2337	07 10 13.60	+44 27 25.0	07 10 12.29	+44 27 43.7	436	9.79	13.48	-16.85	8.10±0.10	1
8	UGC3817	07 22 44.48	+45 06 30.7	07 22 44.84	+45 06 41.8	437	9.82	15.96	-14.44	7.89±0.04	2
9	SDSS	07 23 01.42	+36 21 17.1			885	14.38	17.01	-14.19	7.45±0.15	4d
10	UGC3860	07 28 17.20	+40 46 13.0	07 28 19.44	+40 46 29.9	354	7.81	14.96	-14.75	7.83±0.02	2
11	UGC3876	07 29 17.49	+27 54 01.9	07 29 17.36	+27 53 16.1	854	15.01	13.70	-17.39	7.88±0.04	2
12	SDSS	07 30 58.90	+41 09 59.8	07 30 58.90	+41 09 59.8	874	15.70	16.67	-14.58	8.02±0.03	3
13	SDSS	07 37 28.47	+47 24 32.8			476	10.42	18.06	-12.50	7.28±0.07	4d
14	SDSS	07 44 43.72	+25 08 26.6	07 44 43.72	+25 08 26.6	749	12.95	18.35	-12.39	7.21±0.10	3
15	MCG9-13-56	07 47 32.10	+51 11 29.0	07 47 33.18	+51 11 24.7	439	10.00	15.48	-14.90	7.70±0.03	3,4b
16	UGC4117	07 57 25.98	+35 56 21.0	07 57 26.31	+35 56 19.2	773	14.12	15.34	-15.61	7.82±0.08	2
17	UGC4148	08 00 23.68	+42 11 37.0	08 00 23.68	+42 11 37.0	716	13.55	15.63	-15.21	7.83±0.08	3
18	NGC2500	08 01 53.30	+50 44 15.4	08 01 55.38	+50 44 38.5	504	10.88	12.23	-18.13	8.36±0.03	3
19	MCG7-17-19	08 09 36.10	+41 35 40.0	08 09 37.64	+41 35 29.5	704	13.37	16.65	-14.20	7.96±0.02	2,3
20	SDSS	08 10 30.65	+18 37 04.1	08 10 30.65	+18 37 04.1	1483	23.05	18.29	-13.68	7.79±0.09	3
21	SDSS	08 12 39.53	+48 36 45.4	08 12 39.53	+48 36 45.4	521	11.05	17.23	-13.21	7.27±0.06	4b,3
22	NGC2537	08 13 14.73	+45 59 26.3	08 13 13.05	+45 59 26.3	445	9.86	12.27	-17.93	8.37±0.12	3
23	IC2233	08 13 58.93	+45 44 34.3			553	10.70	13.05	-17.32	8.08±0.19	4a
24	NGC2541	08 14 40.18	+49 03 42.1	08 14 47.53	+49 04 00.0	548	12.00	12.25	-18.36	8.02±0.10	3,4a
25	NGC2552	08 19 20.14	+50 00 25.2			524	11.11	12.92	-17.51	8.28±0.11	4a
26	KUG 0821+321	08 25 04.90	+32 01 05.1	08 25 04.90	+32 01 05.1	648	12.25	16.10	-14.54	7.60±0.03	2
27	HS 0822+3542	08 25 55.43	+35 32 31.9			720	13.49	17.92	-12.93	7.44±0.02	4e
28	SDSS	08 43 37.98	+40 25 47.2	08 43 37.98	+40 25 47.2	614	12.05	17.83	-12.72	7.49±0.03	2,3,4b
29	SDSS	08 52 33.75	+13 50 28.3			1511	23.08	17.43	-14.55	7.28±0.10	4d
30	UGC4704	08 59 00.28	+39 12 35.7	08 59 00.28	+39 12 35.7	596	11.74	15.51	-14.97	7.96±0.05	2
31	SDSS	08 59 46.93	+39 23 05.6			588	11.63	16.98	-13.46	7.57±0.06	4b
32	SDSS	09 11 59.43	+31 35 35.9			750	13.52	17.97	-12.75	7.50±0.05	4b
33	SDSS	09 26 09.45	+33 43 04.1			536	10.63	17.34	-12.90	7.12±0.02	4f
34	SDSS	09 28 59.06	+28 45 28.5	09 28 59.06	+28 45 28.5	1229	19.90	16.70	-14.88	7.68±0.03	3
35	SDSS	09 31 36.15	+27 17 46.6	09 31 36.15	+27 17 46.6	1505	23.60	17.98	-13.96	7.55±0.04	3
36	SDSS	09 40 03.27	+44 59 31.7	09 40 03.27	+44 59 31.7	1246	20.71	17.96	-13.69	7.40±0.03	3
37	KISSB23	09 40 12.67	+29 35 29.3	09 40 12.67	+29 35 29.3	505	10.21	16.32	-13.82	7.60±0.05	3,4b
38	SDSS	09 47 18.35	+41 38 16.4	09 47 18.35	+41 38 16.4	1389	22.56	17.61	-14.22	7.76±0.02	3
39	UGC5272B	09 50 19.49	+31 27 22.3	09 50 19.49	+31 27 22.3	539	10.27	17.68	-12.48	7.60±0.02	2,3
40	UGC5272	09 50 22.40	+31 29 16.0	09 50 21.35	+31 29 16.6	520	10.30	14.46	-15.70	7.84±0.02	2,3
41	SDSS	09 51 41.67	+38 42 07.3	09 51 41.67	+38 42 07.3	1435	23.07	17.42	-14.47	7.85±0.07	3
42	UGC5340	09 56 45.70	+28 49 35.0			502	9.86	14.60	-15.45	7.14±0.03	4b
43	SDSS	10 00 36.50	+30 32 09.8	10 00 36.50	+30 32 09.8	501	9.90	18.06	-12.00	7.42±0.04	2,3
44	UGC5427	10 04 41.05	+29 21 55.2	10 04 40.44	+29 21 35.9	498	9.79	14.89	-15.16	7.90±0.03	2
45	UGC5464	10 08 07.70	+29 32 34.4	10 08 07.70	+29 32 34.4	1003	16.90	15.62	-15.62	7.86±0.04	2
46	SDSS	10 10 14.96	+46 17 44.1	10 10 14.96	+46 17 44.1	1092	18.58	18.20	-13.17	7.78±0.03	3
47	UGC5540	10 16 21.70	+37 46 48.7	10 16 21.70	+37 46 48.7	1162	19.16	14.60	-16.89	8.00±0.10	3
48	HS 1013+3809	10 16 24.50	+37 54 46.0			1173	19.30	15.99	-15.51	7.59±0.04	4g

<sup>†</sup>  $M_{\text{B}}$  from [2]. References for O/H: 1, 2, 3, 4—see table's description. References in parenthesis: a—Kniazev et al. (2004);

b—Izotov &amp; Thuan (2007); c—van Zee (1997); d—Pustilnik et al. (2011); e—Pustilnik et al. (2003a);

f—Pustilnik et al. (2010); g—Kniazev et al. (1999).

galaxies from our recent paper Pustilnik et al. (2011) SDSS J0737+4724 and SDSS J0852+1350 both with 12+log(O/H)=7.28 dex. Finally, for two more Lynx-Cancer void dwarf galaxies, – SDSS J0744+2508 and J0940+4459, we have obtained now a very low oxygen abundance esti-

mate of 12+log(O/H)~7.2–7.4. . Therefore, about a half-dozen of all the 48 void galaxies with known O/H belong to the range of the lowest gas metallicities (12+log(O/H)≲7.3). Out of many thousands of late-type galaxies with known O/H, derived with different methods, only a few such galax-

ies have been found by now (I Zw 18, SBS 0335–052E and W, UGCA 292).

It is worth to compare the surface density of very metal-poor (or eXtremely Metal-Deficient, XMD –  $12 + \log(\text{O}/\text{H}) \leq 7.65$ ) galaxies found in the Lynx-Cancer void sample with the estimates presented by us for two different samples of emission-line galaxies (ELGs). The first estimate was done for the ELG sample from the Hamburg-SAO Survey (HSS) (Ugryumov et al. 1999; Pustilnik et al. 2005, and references therein). Most of these ELGs were selected according to criteria:  $B_{\text{tot}} < 18.5$  and  $\text{EW}([\text{OIII}]\lambda 5007) > 50 \text{ \AA}$ . The latter roughly corresponds to the criterion  $\text{EW}(\text{H}\beta) \gtrsim 10 \text{ \AA}$ . Pustilnik et al. (2003b) have found that the density of XMD galaxies in this sample is about 4 per 1000  $\square^\circ$ . A similar density estimate was derived by Kniazev et al. (2003), based on the galaxy sample selected from the SDSS (roughly similar to the HSS by the limiting  $B$ -magnitude) based on the strength of the  $\text{H}\beta$  emission line ( $\text{EW}(\text{H}\beta) > 10 \text{ \AA}$ ). Both these estimates were based on the XMD galaxies, for which the O/H was derived via the classic  $T_e$ -method.

The region of the celestial sphere, onto which the Lynx-Cancer void in projected contains 19 XMD galaxies, inhabiting this void. Five more XMD galaxies fall in this sky region from both background and foreground. This corresponds to the total surface density of such galaxies of about 10 per 1000  $\square^\circ$ , which is almost a factor of 2.5 larger than the estimates based on the ELG galaxy samples. This can be caused by at least two factors, or a combination therein. The first factor is omission of the selection criterion by rather strong  $\text{H}\beta$  emission. The use of semi-empirical and empirical methods allows one to get more or less reliable estimates of O/H for the cases of relatively weak  $\text{H}\beta$  emission. The second reason is probably directly linked with the fact that a nearby void, populated by a large fraction of dwarf galaxies with slow evolution, is projected onto the given sky region.

The full volume of the Lynx-Cancer void represents only a small fraction (about 5%) of the sphere with  $R = 26 \text{ Mpc}$ , which comprises this void. The existence of such an unusually strong concentration of the most metal-poor galaxies in a small cell of nearby Universe is indicative of the physical relation between the evolutionary status of low-mass late-type galaxies and the type of their global environment. The discovery of several unusual dwarfs with relatively small ages of the oldest visible stellar population among the Lynx-Cancer void objects gives additional evidences for such a relation.

## 5 SUMMARY

1) Based on the results of BTA spectroscopy we present the oxygen abundances for twenty galaxies residing in the nearby Lynx-Cancer void and for nine galaxies situated outside this void. For 14 galaxies, the abundances of oxygen are derived via the classic  $T_e$ -method with the accuracy of O/H varying in the range of 0.06 to 0.15 dex. For the remaining HII regions with a faint or undetected  $[\text{OIII}]\lambda 4363$  line, the abundance of oxygen is estimated via the semi-empirical and empirical methods.

2) For 4 Lynx-Cancer void galaxies with a relatively strong  $[\text{OIII}]\lambda 4363$  line we use the spectra from the SDSS

DR7 database to derive the oxygen abundances via the modified classic  $T_e$  method (from the lines of  $[\text{OII}]\lambda\lambda 7320, 7330$ ). For the remaining 6 galaxies with a faint or undetected  $[\text{OIII}]\lambda 4363$  line, we derive O/H via the empirical methods. We cross-compare all the O/H estimates derived from different measurements (BTA, SDSS and from literature) and via various methods, and calculate the weighted mean value to adopt the most reliable estimate of the galaxy O/H.

3) Combining the data for all 48 galaxies in the Lynx-Cancer void with available O/H and  $M_B$  (including about a dozen of objects from the literature and our other papers), we analyze their locations on the O/H– $M_B$  diagram. A comparison of these data with the linear relationship between  $\log(\text{O}/\text{H})$  and  $M_B$ , derived from three samples of low-mass late-type galaxies residing in the Local Volume and its immediate neighbourhood (the “standard” L–Z relationship) leads to the following conclusions. The first: around 12% of the studied void galaxies (namely, the objects with  $12 + \log(\text{O}/\text{H}) \lesssim 7.3$ ) demonstrate a large oxygen deficiency relative to the abundances, expected from their luminosities in the “standard” L–Z relationship (up to a few times). The second: the majority of the remaining (approximately 88%) void galaxies possess the metal abundances systematically lower than expected from the “standard” L–Z ratio, with the average O/H shift of the group amounting to about 0.12 dex (or around 30 %).

4) A significant concentration of the most metal-poor dwarf galaxies with  $M_B$  ranging from  $-12$  to  $-15.5 \text{ mag}$  is discovered in the small cell of the Local Supercluster, which includes the Lynx-Cancer void. This provides the evidence for the sizable effect of a very rarefied environment on the evolution of low-mass galaxies.

## ACKNOWLEDGEMENTS

The authors thank S. Kaisin for providing the  $\text{H}\alpha$  images of several program galaxies prior to the publication. The work of S. Pustilnik and A. Tepliakova was partly supported by the RFSB grants (project nos. 06-02-16617 and 10-02-92650), as well as the Federal Target Programm Scientific and Scientific-Pedagogical Cadre of Innovative Russia (state contract no. 14.740.11.0901). A. Kniazev acknowledges the support from the National Research Foundation of South Africa. We thank A. Burenkov and A. Valeev for the help with observations. We also thank N. G. Guseva for the constructive comments and suggestions that improved the quality of the paper. The authors acknowledge the spectral and photometric data used for this study and the related information available in the SDSS database. The Sloan Digital Sky Survey (SDSS) is a joint project of the University of Chicago (Fermilab), the Institute for Advanced Study, the Japan Participation Group, the John Hopkins University, the Max-Planck-Institute for Astronomy (MPIA), the Max-Planck-Institute for Astrophysics (MPA), New Mexico State University, Princeton University, the United States Naval Observatory, and the University of Washington. The Apache Point Observatory, site of the SDSS telescopes, is operated by the Astrophysical Research Consortium (ARC). This research has made use of the NASA/IPAC Extragalactic Database (NED), which is operated by the Jet Propulsion Laboratory, California Institute of Technology under



contract with the National Aeronautics and Space Administration, and the HyperLeda database, which is operated by Lyon University.

## REFERENCES

- Abazajian K.N., Adelman-McCarthy J.K., Agüeros M.A., et al., 2009, *ApJS*, 182, 543
- Afanasiev V.L., Moiseev A.V., 2005, *Astron. Lett.*, 31, 193
- Afanasiev V.L., Burenkov A.N., Vlasyuk V.V., Drabek S.V., 1995, SAO RAS Internal report No. 234
- Aller H.L., 1984, *Physics of Thermal Gaseous Nebulae*, Dordrecht, Reidel
- Bohlin R.C., 1996, *AJ*, 111, 1743
- Gunn J.E., Carr M.A., Rockosi C.M. et al., 1998, *AJ*, 116, 3040
- Guseva N.G., Papaderos P., Izotov Y.I., Green R.F., Fricke K.J., Thuan T.X., Noeske K.G., 2003, *A&A*, 407, 105
- Guseva N.G., Papaderos P., Meyer H.T., Izotov Y.I., Fricke K.J., 2009, *A&A*, 505, 63
- Izotov Y.I., Thuan T.X., 2007, *ApJ*, 665, 1115
- Izotov Y.I., Thuan T.X., Lipovetsky V.A., 1994, *ApJ*, 435, 647
- Izotov Y.I., Stasinska G., Meynet G., et al., 2006, *A&A*, 448, 955
- Izotov Y.I., Guseva N.G., Fricke K.J., Papaderos P., 2009, *A&A*, 503, 611
- Karachentsev I.D., Kaisin S.S., 2010, *AJ*, 140, 1241
- Lee H., MacCall M.L., Kingsburgh R.L., Ross R., & Steveson C.C., 2003, *AJ*, 125, 146
- Kniazev A.Y., Pustilnik S.A., Ugryumov A.V., 1999, *Bulletin SAO*, 46, 23
- Kniazev A.Y., Grebel E.K., Hao L., Strauss M., Brinkmann J., Fukugita M., 2003, *ApJ*, 593, L73
- Kniazev A.Y., Pustilnik S.A., Grebel E.K., Lee H., Pramskij A.G., 2004, *ApJS*, 153, 429
- Kniazev A.Y., et al. 2008, *MNRAS*, 388, 1667
- Papaderos P., Loose H.-H., Fricke K.J., Thuan T.X., 1996, *A&A*, 314, 59
- Peebles P.J.E., 2001, *ApJ*, 557, 459
- Pilyugin L.S., Vilchez J.M., Thuan T.X., 2010, *ApJ*, 720, 1738
- Pilyugin L., Mattsson L., 2011, *MNRAS*, 412, 1145
- Pustilnik S.A., Tepliakova A.L., 2011, *MNRAS*, 415, 954
- Pustilnik S.A., Kniazev A.Y., Pramsky A.G., Ugryumov A.V., Masegosa J., 2003a, *A&A*, 409, 917
- Pustilnik S.A., Kniazev A.Y., Pramsky A.G., Ugryumov A.V., 2003b, *Ap.Spa.Sci.*, 284, 795
- Pustilnik S.A., Kniazev A.Y., Pramsky A.G., Izotov Y.I., Foltz C., Brosch N., Martin J.-M., Ugryumov A., 2004a, *A&A*, 419, 469
- Pustilnik S.A., Pramsky A.G., Kniazev A.Y., 2004b, *A&A*, 425, 51
- Pustilnik S.A., Engels D., Lipovetsky V.A., Kniazev A.Y., Pramsky A.G., Ugryumov A.V., et al. 2005, *A&A*, 442, 109
- Pustilnik S.A., Kniazev A.Y., Pramskij A.G. 2005, *A&A*, 443, 91
- Pustilnik S.A., Engels D., Kniazev A.Y., Pramskij A.G., Ugryumov A.V., Hagen H.-J., 2006, *Astron.Lett.* 32, 228
- Pustilnik S.A., Tepliakova A.L., Kniazev A.Y., 2008, *Pis'ma v AZh*, 34, 503 = *Astron.Lett.*, 34, 457 (arXiv:/0712.4007)
- Pustilnik S.A., Tepliakova A.L., Kniazev A.Y., Burenkov A.N., 2010, *MNRAS*, 401, 333
- Pustilnik S.A., Martin J.-M., Tepliakova A.L., Kniazev A.Y., 2011, *MNRAS*, in press
- Ugryumov A.V., Engels D., Lipovetsky V.A., et al. 1999, *A&A*, 374, 907
- van Zee L., 1997, *AJ*, 119, 2757
- van Zee L., 2000, *ApJ Lett.*, 543, L31
- van Zee L., Haynes M.P. 2006, *ApJ*, 636, 214
- van Zee L., Skillman E., Haynes M.P. 2006, 637, 269

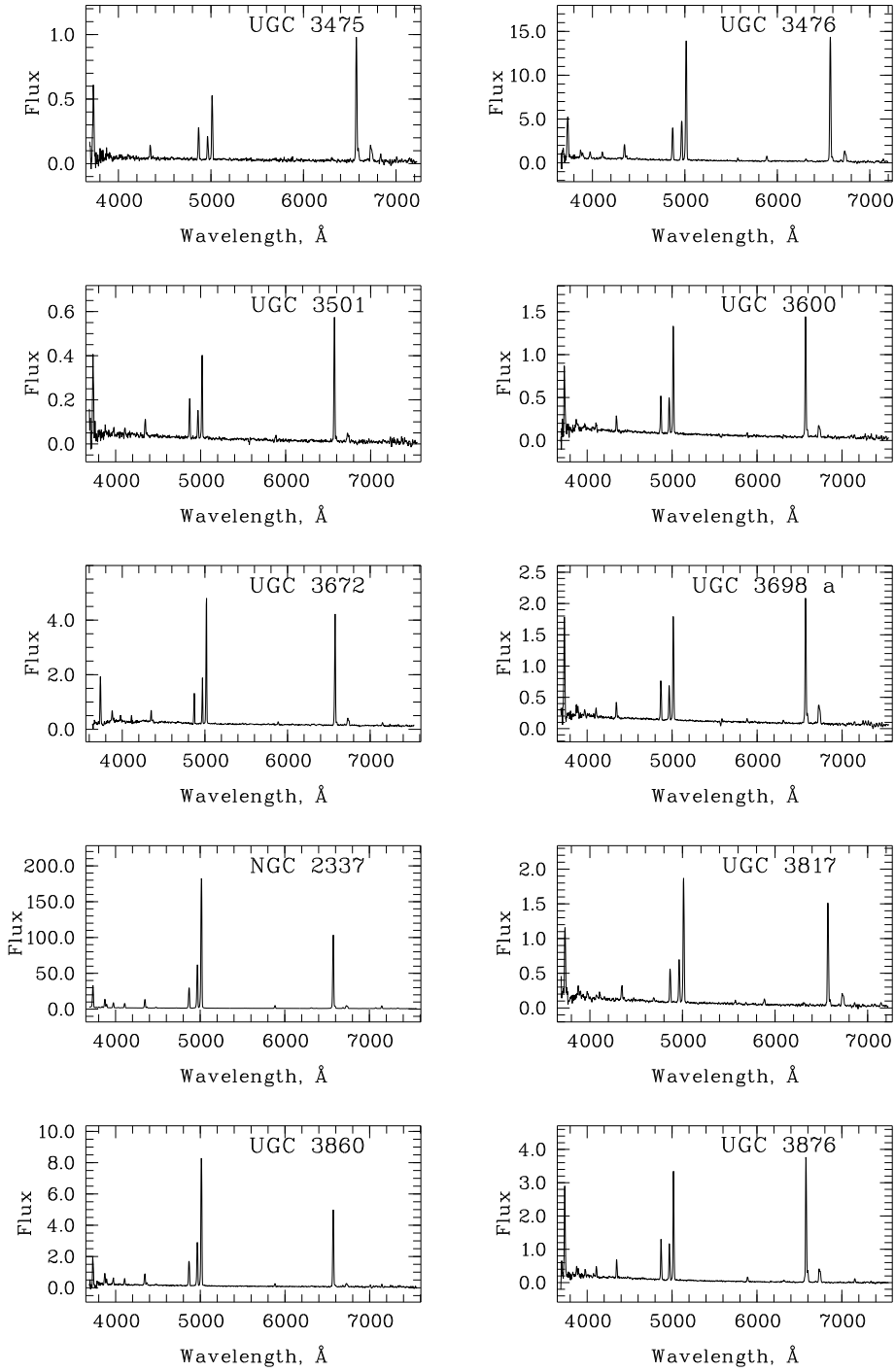


**Figure 4.** Figure A.1. Spectra of 10 HII regions in the Lynx-Cancer void galaxies obtained with the SAO 6m telescope.

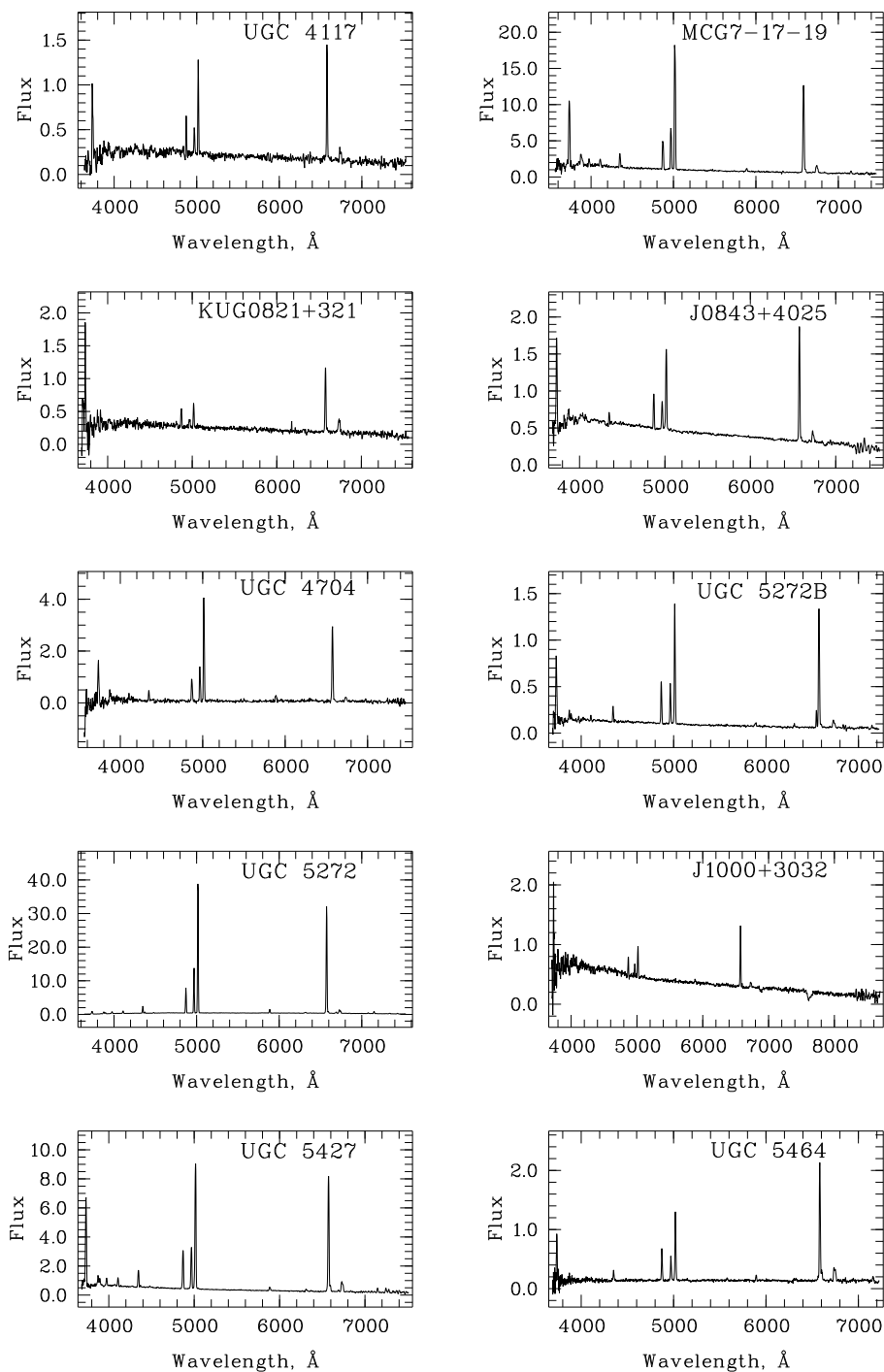


**Figure 5.** Figure A.2. Spectra of 10 HII regions in the remaining Lynx-Cancer void galaxies obtained with the SAO 6m telescope.

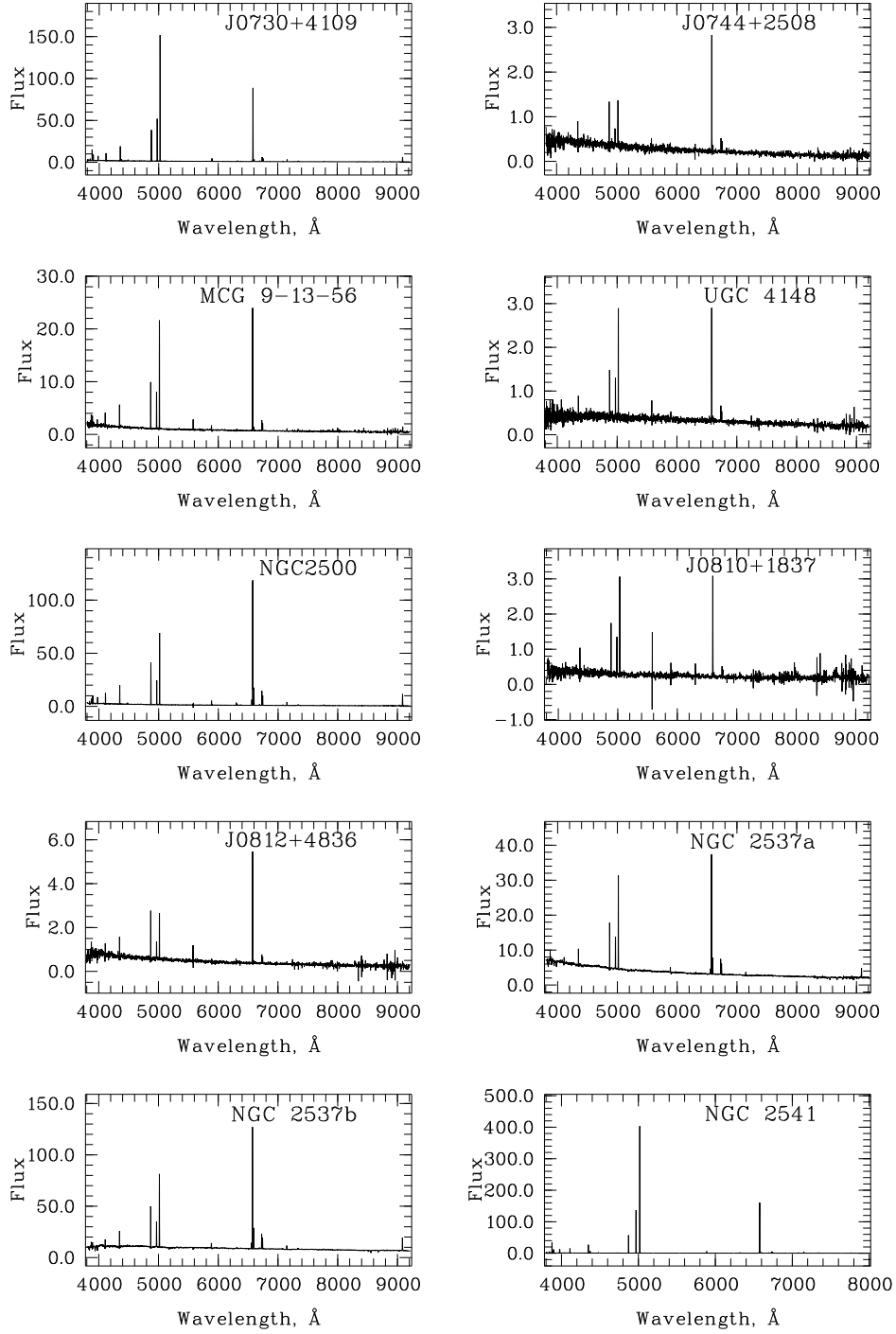


Figure 6. Figure A.3. Spectra of 10 HII regions in the Lynx-Cancer void galaxies obtained from SDSS DR7.

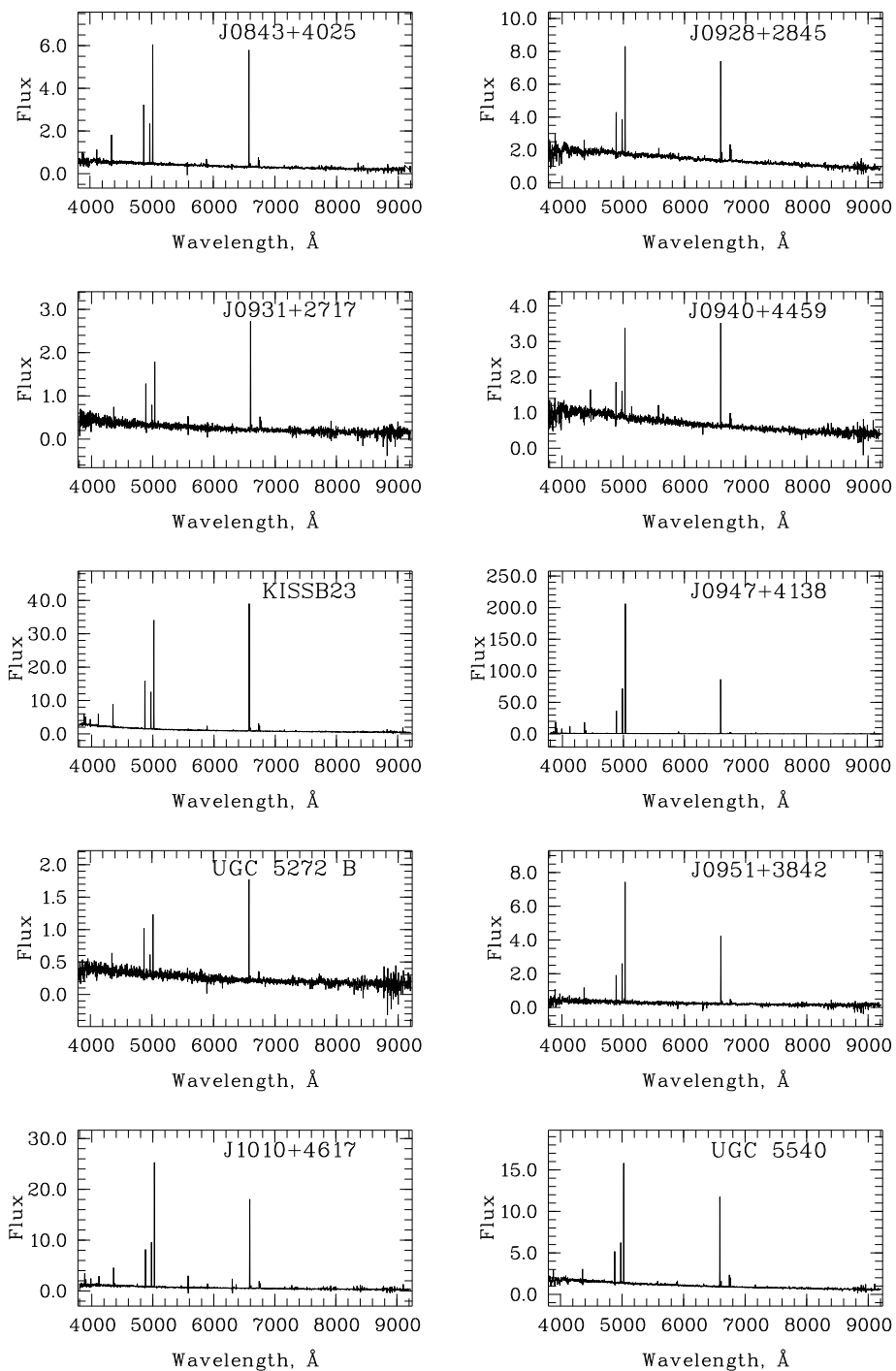
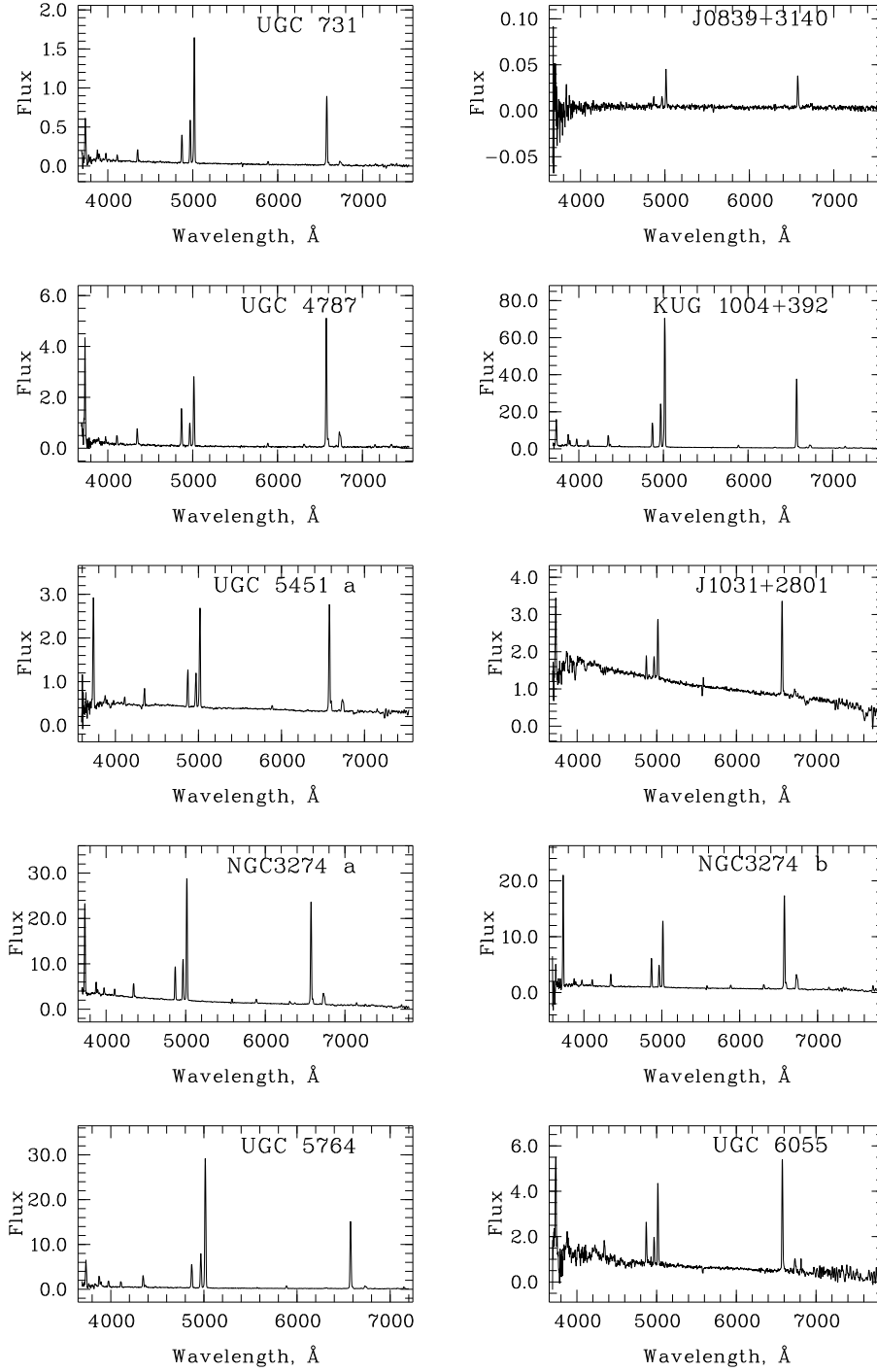


Figure 7. Figure A.4. Spectra of other 8 HII regions in the Lynx-Cancer void galaxies obtained from the SDSS.



**Figure 8.** Figure A.5. Spectra of 10 HII regions in 9 galaxies outside the Lynx-Cancer void obtained with the SAO 6m telescope.

**Table 3. Table B.1** Observed and corrected relative fluxes in the lines of void galaxies (BTA)

$\lambda_0(\text{\AA})$ Ion	UGC3475		UGC3476		UGC3501	
	F( $\lambda$ )/F(H $\beta$ )	I( $\lambda$ )/I(H $\beta$ )	F( $\lambda$ )/F(H $\beta$ )	I( $\lambda$ )/I(H $\beta$ )	F( $\lambda$ )/F(H $\beta$ )	I( $\lambda$ )/I(H $\beta$ )
3727 [O II]	2.852± 0.235	4.460± 0.378	1.160± 0.053	1.576± 0.074	2.216± 0.118	2.312± 0.140
3868 [Ne III]	...	...	0.162± 0.016	0.210± 0.021	0.168± 0.026	0.172± 0.030
3967 [Ne III] + H7	...	...	0.214± 0.013	0.275± 0.022	0.112± 0.022	0.234± 0.055
4101 H $\delta$	...	...	0.198± 0.012	0.246± 0.020	0.112± 0.018	0.228± 0.044
4340 H $\gamma$	0.426± 0.159	0.518± 0.239	0.416± 0.017	0.478± 0.023	0.418± 0.033	0.498± 0.044
4363 [O III]	0.029± 0.100	0.035± 0.121	0.068± 0.011	0.077± 0.013	0.052± 0.022	0.050± 0.023
4861 H $\beta$	1.000± 0.046	1.000± 0.130	1.000± 0.030	1.000± 0.031	1.000± 0.049	1.000± 0.053
4959 [O III]	0.674± 0.039	0.650± 0.038	1.198± 0.037	1.168± 0.037	0.586± 0.029	0.535± 0.029
5007 [O III]	2.155± 0.087	2.045± 0.083	3.720± 0.105	3.587± 0.103	1.957± 0.083	1.779± 0.082
5876 He I	0.048± 0.016	0.035± 0.012	0.154± 0.014	0.124± 0.011	0.134± 0.026	0.113± 0.024
6300 [O I]	...	...	0.061± 0.011	0.045± 0.008	...	...
6312 [S III]	...	...	0.012± 0.009	0.009± 0.007	...	...
6548 [N II]	0.113± 0.026	0.070± 0.016	0.027± 0.007	0.019± 0.005	0.022± 0.013	0.017± 0.011
6563 H $\alpha$	4.590± 0.167	2.818± 0.120	3.901± 0.099	2.792± 0.078	3.388± 0.132	2.756± 0.126
6584 [N II]	0.377± 0.053	0.231± 0.033	0.072± 0.024	0.052± 0.018	0.090± 0.030	0.073± 0.027
6717 [S II]	0.506± 0.042	0.300± 0.026	0.294± 0.013	0.205± 0.009	0.203± 0.027	0.162± 0.024
6731 [S II]	0.368± 0.041	0.217± 0.025	0.133± 0.009	0.093± 0.007	0.168± 0.026	0.134± 0.023
C(H $\beta$ ), dex	0.64±0.05		0.43±0.03		0.17±0.05	
EW(abs), $\text{\AA}$	0.20±8.76		0.40±1.17		5.60±0.12	
F(H $\beta$ )	3.10±0.10		55.3±1.0		2.32±0.08	
EW(H $\beta$ ), $\text{\AA}$	73± 2		169± 4		66± 2	
Rad. vel., km s $^{-1}$	347±27		423±21		563±30	

**Table 4. Table B.2** Observed and corrected relative fluxes in the lines of void galaxies (BTA)

$\lambda_0(\text{\AA})$ Ion	UGC3600		UGC3672		UGC3698a	
	F( $\lambda$ )/F(H $\beta$ )	I( $\lambda$ )/I(H $\beta$ )	F( $\lambda$ )/F(H $\beta$ )	I( $\lambda$ )/I(H $\beta$ )	F( $\lambda$ )/F(H $\beta$ )	I( $\lambda$ )/I(H $\beta$ )
3727 [O II]	1.496± 0.099	1.636± 0.116	1.893± 0.089	2.848± 0.145	2.836± 0.105	3.177± 0.132
3868 [Ne III]	0.261± 0.027	0.280± 0.031	0.442± 0.041	0.627± 0.060	0.254± 0.025	0.278± 0.029
3967 [Ne III] + H7	0.140± 0.028	0.235± 0.056	0.186± 0.026	0.259± 0.055	0.106± 0.011	0.208± 0.026
4101 H $\delta$	0.130± 0.022	0.218± 0.044	0.222± 0.028	0.292± 0.049	0.169± 0.009	0.261± 0.018
4340 H $\gamma$	0.445± 0.027	0.507± 0.035	0.408± 0.030	0.488± 0.049	0.400± 0.015	0.473± 0.020
4363 [O III]	0.051± 0.018	0.051± 0.019	0.064± 0.018	0.076± 0.022	0.057± 0.008	0.058± 0.009
4861 H $\beta$	1.000± 0.037	1.000± 0.040	1.000± 0.058	1.000± 0.063	1.000± 0.035	1.000± 0.037
4959 [O III]	0.933± 0.035	0.879± 0.035	1.350± 0.070	1.306± 0.068	0.891± 0.029	0.832± 0.029
5007 [O III]	2.903± 0.092	2.724± 0.091	4.263± 0.203	4.062± 0.196	2.703± 0.080	2.507± 0.079
5876 He I	0.051± 0.012	0.044± 0.011	0.126± 0.018	0.094± 0.014	0.069± 0.006	0.058± 0.005
6548 [N II]	0.046± 0.012	0.038± 0.010	0.046± 0.012	0.029± 0.008	0.070± 0.007	0.055± 0.006
6563 H $\alpha$	3.388± 0.103	2.800± 0.098	4.388± 0.194	2.809± 0.137	3.502± 0.100	2.781± 0.092
6584 [N II]	0.161± 0.032	0.132± 0.027	0.155± 0.045	0.099± 0.029	0.228± 0.031	0.179± 0.026
6717 [S II]	0.304± 0.021	0.247± 0.018	0.306± 0.026	0.190± 0.017	0.512± 0.018	0.398± 0.016
6731 [S II]	0.230± 0.021	0.186± 0.018	0.182± 0.023	0.113± 0.015	0.354± 0.015	0.274± 0.013
7136 [Ar III]	...	...	0.126± 0.020	0.072± 0.012	0.064± 0.008	0.048± 0.007
C(H $\beta$ ), dex	0.20±0.04		0.58±0.06		0.24±0.04	
EW(abs), $\text{\AA}$	3.65±0.68		0.15±1.14		3.40±0.29	
F(H $\beta$ )	6.09±0.15		11.53±0.47		8.57±0.19	
EW(H $\beta$ ), $\text{\AA}$	73± 2		51± 2		58± 1	
Rad. vel., km s $^{-1}$	419±33		627±45		403±30	

**Table 5. Table B.3** Observed and corrected relative fluxes in the lines of void galaxies (BTA)

$\lambda_0(\text{\AA})$ Ion	UGC3698b		NGC2337		UGC3817	
	F( $\lambda$ )/F(H $\beta$ )	I( $\lambda$ )/I(H $\beta$ )	F( $\lambda$ )/F(H $\beta$ )	I( $\lambda$ )/I(H $\beta$ )	F( $\lambda$ )/F(H $\beta$ )	I( $\lambda$ )/I(H $\beta$ )
3727 [O II]	3.361±0.240	4.082±0.341	1.054±0.029	1.270±0.038	2.174±0.125	2.406±0.152
3868 [Ne III]	0.426±0.063	0.496±0.083	0.414±0.011	0.485±0.014	0.335±0.084	0.362±0.096
3967 [Ne III] + H7	...	...	0.251±0.007	0.318±0.012	0.171±0.070	0.274±0.130
4101 H $\delta$	0.118±0.030	0.274±0.086	0.203±0.007	0.257±0.011	0.081±0.049	0.175±0.129
4340 H $\gamma$	0.355±0.045	0.479±0.070	0.413±0.013	0.467±0.016	0.498±0.032	0.568±0.044
4363 [O III]	0.106±0.036	0.109±0.041	0.043±0.006	0.045±0.007	0.063±0.020	0.064±0.021
4740 [Ar IV]	...	...	0.004±0.001	0.004±0.001	...	...
4861 H $\beta$	1.000±0.075	1.000±0.084	1.000±0.029	1.000±0.030	1.000±0.044	1.000±0.050
4959 [O III]	0.787±0.059	0.697±0.058	2.116±0.067	2.043±0.066	1.298±0.050	1.210±0.049
5007 [O III]	2.479±0.150	2.172±0.146	6.441±0.183	6.173±0.179	4.088±0.147	3.789±0.145
5876 He I	0.071±0.024	0.052±0.020	0.137±0.004	0.117±0.004	0.197±0.022	0.166±0.020
6300 [O I]	...	...	0.030±0.002	0.024±0.002	0.049±0.020	0.040±0.017
6312 [S III]	...	...	0.011±0.002	0.009±0.001	0.059±0.020	0.048±0.017
6364 [O I]	...	...	0.011±0.001	0.008±0.001	...	...
6548 [N II]	0.071±0.036	0.047±0.026	0.030±0.001	0.024±0.001	0.047±0.016	0.037±0.014
6563 H $\alpha$	4.012±0.231	2.683±0.187	3.646±0.090	2.874±0.079	3.517±0.124	2.810±0.115
6584 [N II]	0.248±0.061	0.163±0.044	0.090±0.026	0.071±0.021	0.159±0.039	0.126±0.033
6678 He I	...	...	0.038±0.002	0.029±0.001	0.024±0.008	0.019±0.007
6717 [S II]	0.604±0.073	0.389±0.053	0.140±0.005	0.108±0.004	0.400±0.077	0.314±0.065
6731 [S II]	0.207±0.054	0.133±0.039	0.094±0.004	0.073±0.004	0.301±0.082	0.236±0.068
7136 [Ar III]	...	...	0.129±0.004	0.096±0.003	0.083±0.017	0.063±0.013
C(H $\beta$ ), dex	0.41±0.07		0.29±0.03		0.23±0.05	
EW(abs), $\text{\AA}$	2.35±0.09		5.90±1.25		3.40±1.03	
F(H $\beta$ )	1.69±0.09		415±8		6.15±0.18	
EW(H $\beta$ ), $\text{\AA}$	22±1		293±6		57±2	
Rad. vel., km s $^{-1}$	325±87		451±9		369±36	

**Table 6. Table B.4** Observed and corrected relative fluxes in the lines of void galaxies (BTA)

$\lambda_0(\text{\AA})$ Ion	UGC3860		UGC3876		UGC4117	
	F( $\lambda$ )/F(H $\beta$ )	I( $\lambda$ )/I(H $\beta$ )	F( $\lambda$ )/F(H $\beta$ )	I( $\lambda$ )/I(H $\beta$ )	F( $\lambda$ )/F(H $\beta$ )	I( $\lambda$ )/I(H $\beta$ )
3727 [O II]	1.029±0.059	1.147±0.067	2.235±0.098	2.514±0.115	2.902±0.300	3.466±0.384
3868 [Ne III]	0.451±0.019	0.495±0.021	0.199±0.017	0.220±0.019	...	...
3967 [Ne III] + H7	0.222±0.016	0.243±0.022	0.160±0.015	0.189±0.022	...	...
4101 H $\delta$	0.222±0.012	0.240±0.017	0.232±0.013	0.262±0.020	...	...
4340 H $\gamma$	0.482±0.021	0.506±0.024	0.438±0.018	0.469±0.022	...	...
4363 [O III]	0.106±0.014	0.110±0.015	0.034±0.012	0.035±0.013	...	...
4471 He I	0.031±0.009	0.032±0.009	...	...	...	...
4861 H $\beta$	1.000±0.035	1.000±0.036	1.000±0.034	1.000±0.034	1.000±0.091	1.000±0.109
4959 [O III]	1.730±0.058	1.713±0.057	0.910±0.031	0.896±0.031	0.804±0.073	0.767±0.072
5007 [O III]	5.148±0.156	5.079±0.154	2.777±0.085	2.721±0.084	2.528±0.235	2.393±0.231
5876 He I	0.101±0.011	0.093±0.010	0.113±0.010	0.103±0.009	...	...
6548 [N II]	0.014±0.008	0.012±0.007	0.097±0.011	0.085±0.010	0.029±0.031	0.022±0.025
6563 H $\alpha$	3.141±0.091	2.787±0.088	3.256±0.094	2.831±0.090	3.586±0.244	2.793±0.216
6584 [N II]	0.046±0.026	0.041±0.023	0.299±0.036	0.259±0.032	0.100±0.047	0.077±0.038
6717 [S II]	0.146±0.013	0.128±0.012	0.345±0.016	0.297±0.015	0.361±0.062	0.275±0.050
6731 [S II]	0.062±0.012	0.054±0.011	0.278±0.016	0.239±0.014	0.236±0.053	0.179±0.043
7136 [Ar III]	0.098±0.009	0.084±0.008	0.091±0.009	0.076±0.008	...	...
C(H $\beta$ ), dex	0.15±0.04		0.17±0.04		0.29±0.09	
EW(abs), $\text{\AA}$	0.25±1.23		0.95±0.95		0.70±1.18	
F(H $\beta$ )	23.48±0.54		16.53±0.34		000±0	
EW(H $\beta$ ), $\text{\AA}$	173±4		147±4		22±1	
Rad. vel., km s $^{-1}$	319±36		609±60		684±27	



**Table 7. Table B.5** Observed and corrected relative fluxes in the lines of void galaxies (BTA)

$\lambda_0(\text{\AA})$ Ion	MCG7-17-19		KUG0821+321		J0843+4025	
	F( $\lambda$ )/F(H $\beta$ )	I( $\lambda$ )/I(H $\beta$ )	F( $\lambda$ )/F(H $\beta$ )	I( $\lambda$ )/I(H $\beta$ )	F( $\lambda$ )/F(H $\beta$ )	I( $\lambda$ )/I(H $\beta$ )
3727 [O II]	2.401± 0.105	2.840± 0.133	3.548± 0.467	3.509± 0.564	2.244± 0.092	1.616± 0.099
3868 [Ne III]	0.638± 0.060	0.736± 0.070	...	...	...	...
3967 [Ne III] + H7	0.274± 0.036	0.316± 0.053	...	...	...	...
4101 H $\delta$	0.258± 0.031	0.290± 0.048	...	...	...	...
4340 H $\gamma$	0.451± 0.024	0.487± 0.038	...	...	0.198± 0.020	0.470± 0.079
4363 [O III]	0.081± 0.021	0.086± 0.023	...	...	0.047± 0.019	0.034± 0.019
4861 H $\beta$	1.000± 0.044	1.000± 0.049	1.000± 0.156	1.000± 0.202	1.000± 0.047	1.000± 0.067
4959 [O III]	1.369± 0.062	1.349± 0.062	0.474± 0.129	0.410± 0.128	0.861± 0.039	0.618± 0.039
5007 [O III]	4.227± 0.193	4.138± 0.190	1.143± 0.166	0.985± 0.165	2.556± 0.100	1.834± 0.100
5876 He I	0.111± 0.016	0.099± 0.015	...	...	...	...
6548 [N II]	0.030± 0.000	0.025± 0.000	0.047± 0.084	0.036± 0.073	0.024± 0.016	0.017± 0.016
6563 H $\alpha$	3.360± 0.124	2.791± 0.113	3.516± 0.413	2.767± 0.409	3.658± 0.134	2.798± 0.155
6584 [N II]	0.093± 0.000	0.077± 0.000	0.162± 0.110	0.124± 0.096	0.080± 0.033	0.057± 0.033
6717 [S II]	0.387± 0.025	0.317± 0.021	0.853± 0.169	0.645± 0.152	0.323± 0.023	0.231± 0.024
6731 [S II]	...	...	0.339± 0.133	0.256± 0.117	0.154± 0.020	0.110± 0.020
7136 [Ar III]	0.103± 0.017	0.082± 0.014	...	...	...	...
C(H $\beta$ ), dex	0.24±0.05		0.17±0.15		0.01±0.05	
EW(abs), $\text{\AA}$	0.15±1.28		2.30±1.46		5.00±0.13	
F(H $\beta$ )	64.9±1.9		4.07±0.45		6.35±0.21	
EW(H $\beta$ ), $\text{\AA}$	62± 2		16± 2		13± 0	
Rad. vel., km s $^{-1}$	712±132		673±138		533±21	

**Table 8. Table B.6** Observed and corrected relative fluxes in the lines of void galaxies (BTA)

$\lambda_0(\text{\AA})$ Ion	UGC4704		UGC5272B		UGC5272	
	F( $\lambda$ )/F(H $\beta$ )	I( $\lambda$ )/I(H $\beta$ )	F( $\lambda$ )/F(H $\beta$ )	I( $\lambda$ )/I(H $\beta$ )	F( $\lambda$ )/F(H $\beta$ )	I( $\lambda$ )/I(H $\beta$ )
3727 [O II]	1.927± 0.165	2.252± 0.206	1.585± 0.108	1.543± 0.124	1.209± 0.026	1.503± 0.039
3868 [Ne III]	...	...	0.253± 0.079	0.242± 0.087	0.397± 0.022	0.479± 0.027
3967 [Ne III] + H7	...	...	...	...	0.268± 0.010	0.320± 0.015
4101 H $\delta$	...	...	0.078± 0.008	0.251± 0.038	0.245± 0.009	0.285± 0.014
4340 H $\gamma$	0.403± 0.039	0.459± 0.058	0.367± 0.021	0.481± 0.033	0.471± 0.014	0.519± 0.017
4363 [O III]	0.058± 0.026	0.061± 0.028	0.054± 0.014	0.049± 0.015	0.081± 0.009	0.088± 0.010
4861 H $\beta$	1.000± 0.060	1.000± 0.072	1.000± 0.040	1.000± 0.046	1.000± 0.018	1.000± 0.019
4959 [O III]	1.406± 0.089	1.333± 0.088	0.966± 0.038	0.829± 0.037	1.624± 0.089	1.595± 0.088
5007 [O III]	4.398± 0.236	4.140± 0.232	3.030± 0.106	2.591± 0.105	4.958± 0.117	4.829± 0.115
5876 He I	0.396± 0.049	0.333± 0.043	...	...	0.123± 0.005	0.105± 0.004
6300 [O I]	...	...	0.070± 0.014	0.054± 0.013	...	...
6312 [S III]	...	...	0.008± 0.010	0.006± 0.009	...	...
6548 [N II]	0.020± 0.015	0.016± 0.012	0.020± 0.012	0.015± 0.011	0.016± 0.003	0.013± 0.002
6563 H $\alpha$	3.595± 0.164	2.823± 0.147	3.581± 0.134	2.798± 0.131	3.562± 0.117	2.805± 0.101
6584 [N II]	0.068± 0.034	0.053± 0.027	0.078± 0.058	0.060± 0.051	0.049± 0.015	0.039± 0.012
6717 [S II]	0.334± 0.043	0.256± 0.035	0.212± 0.019	0.161± 0.017	0.124± 0.008	0.096± 0.006
6731 [S II]	...	...	0.128± 0.018	0.097± 0.016	0.082± 0.008	0.063± 0.006
7136 [Ar III]	...	...	...	...	0.086± 0.004	0.063± 0.003
C(H $\beta$ ), dex	0.28±0.06		0.17±0.05		0.31±0.04	
EW(abs), $\text{\AA}$	7.00±6.14		6.60±0.11		0.40±0.94	
F(H $\beta$ )	12.88±0.53		4.99±0.13		000±0	
EW(H $\beta$ ), $\text{\AA}$	175± 7		43± 1		182± 2	
Rad. vel., km s $^{-1}$	480±87		359±54		595±21	

**Table 9. Table B.7** Observed and corrected relative fluxes in the lines of void galaxies (BTA)

$\lambda_0(\text{\AA})$ Ion	J1000+3032		—		UGC5427		UGC5464	
	F( $\lambda$ )/F(H $\beta$ )	I( $\lambda$ )/I(H $\beta$ )	F( $\lambda$ )/F(H $\beta$ )	I( $\lambda$ )/I(H $\beta$ )	F( $\lambda$ )/F(H $\beta$ )	I( $\lambda$ )/I(H $\beta$ )	F( $\lambda$ )/F(H $\beta$ )	I( $\lambda$ )/I(H $\beta$ )
3727 [O II]	2.574± 0.393	1.963± 0.431	2.193± 0.066	2.202± 0.073	1.451± 0.078	2.224± 0.123	...	...
3967 [Ne III] + H7	...	...	0.180± 0.008	0.251± 0.015	...	...	...	...
4101 H $\delta$	...	...	0.187± 0.008	0.252± 0.014	...	...	...	...
4340 H $\gamma$	...	...	0.422± 0.014	0.471± 0.018	0.388± 0.022	0.470± 0.034	...	...
4363 [O III]	...	...	0.040± 0.008	0.039± 0.008	0.023± 0.012	0.027± 0.015	...	...
4861 H $\beta$	1.000± 0.123	1.000± 0.190	1.000± 0.030	1.000± 0.032	1.000± 0.030	1.000± 0.036	...	...
4959 [O III]	0.590± 0.090	0.422± 0.090	1.114± 0.033	1.057± 0.033	0.787± 0.025	0.758± 0.025	...	...
5007 [O III]	1.926± 0.204	1.374± 0.203	3.361± 0.100	3.182± 0.100	2.329± 0.063	2.209± 0.061	...	...
5876 He I	0.164± 0.078	0.113± 0.075	0.092± 0.008	0.084± 0.007	0.154± 0.011	0.113± 0.008	...	...
6300 [O I]	...	...	...	...	0.075± 0.018	0.050± 0.012	...	...
6312 [S III]	...	...	...	...	0.073± 0.018	0.049± 0.012	...	...
6548 [N II]	0.053± 0.077	0.036± 0.072	0.042± 0.006	0.037± 0.006	0.129± 0.011	0.081± 0.007	...	...
6563 H $\alpha$	3.889± 0.364	2.775± 0.396	3.125± 0.082	2.835± 0.085	4.556± 0.117	2.846± 0.082	...	...
6584 [N II]	0.172± 0.096	0.116± 0.091	0.127± 0.029	0.114± 0.027	0.407± 0.041	0.253± 0.026	...	...
6717 [S II]	0.347± 0.107	0.232± 0.101	0.286± 0.012	0.256± 0.012	0.512± 0.022	0.309± 0.014	...	...
6731 [S II]	0.222± 0.100	0.149± 0.094	0.175± 0.011	0.157± 0.011	0.446± 0.021	0.268± 0.013	...	...
7136 [Ar III]	...	...	0.085± 0.006	0.075± 0.006	0.121± 0.013	0.067± 0.007	...	...
C(H $\beta$ ), dex	0.09±0.12	...	0.07±0.03	...	0.61±0.03	...	...	...
EW(abs), $\text{\AA}$	3.15±0.58	...	4.25±0.43	...	0.20±0.73	...	...	...
F(H $\beta$ )	3.78±0.33	...	38.7±0.7	...	6.72±0.10	...	...	...
EW(H $\beta$ ), $\text{\AA}$	8± 1	...	85± 2	...	38± 1	...	...	...
Rad. vel., km s <sup>-1</sup>	459±27	...	495±21	...	831±81	...	...	...

**Table 10. Table B.8** Observed and corrected relative fluxes in the lines of void galaxies (SDSS)

$\lambda_0(\text{\AA})$ Ion	J0730+4109		J0744+2508		MCG9-13-56	
	F( $\lambda$ )/F(H $\beta$ )	I( $\lambda$ )/I(H $\beta$ )	F( $\lambda$ )/F(H $\beta$ )	I( $\lambda$ )/I(H $\beta$ )	F( $\lambda$ )/F(H $\beta$ )	I( $\lambda$ )/I(H $\beta$ )
(3727 [O II])	...	...	1.143± 0.865	0.946± 0.963	1.905± 0.235	2.043± 0.264
3868 [Ne III]	0.347± 0.014	0.408± 0.017	...	...	0.185± 0.045	0.196± 0.050
4101 H $\delta$	0.220± 0.010	0.253± 0.015	...	...	0.210± 0.017	0.280± 0.030
4340 H $\gamma$	0.457± 0.014	0.498± 0.018	0.210± 0.061	0.470± 0.220	0.407± 0.022	0.466± 0.031
4363 [O III]	0.054± 0.007	0.058± 0.008	...	...	...	...
4471 He I	0.035± 0.004	0.038± 0.005	0.068± 0.049	0.052± 0.051	0.025± 0.010	0.024± 0.010
4861 H $\beta$	1.000± 0.021	1.000± 0.022	1.000± 0.166	1.000± 0.231	1.000± 0.029	1.000± 0.033
4959 [O III]	1.480± 0.041	1.454± 0.041	0.402± 0.126	0.298± 0.126	0.787± 0.027	0.750± 0.027
5007 [O III]	4.666± 0.129	4.552± 0.127	1.069± 0.171	0.790± 0.169	2.463± 0.066	2.338± 0.065
5876 He I	0.109± 0.004	0.095± 0.004	...	...	0.092± 0.017	0.082± 0.016
6300 [O I]	0.030± 0.004	0.025± 0.004	...	...	0.030± 0.007	0.026± 0.006
6312 [S III]	0.017± 0.004	0.014± 0.003	...	...	...	...
6548 [N II]	0.032± 0.002	0.026± 0.002	0.039± 0.035	0.026± 0.032	0.025± 0.005	0.021± 0.005
6563 H $\alpha$	3.494± 0.089	2.834± 0.079	3.853± 0.460	2.718± 0.473	3.226± 0.076	2.777± 0.075
6584 [N II]	0.097± 0.006	0.078± 0.005	0.125± 0.043	0.083± 0.039	0.080± 0.007	0.068± 0.006
6717 [S II]	0.202± 0.006	0.162± 0.005	0.496± 0.082	0.329± 0.077	0.282± 0.011	0.238± 0.010
6731 [S II]	0.144± 0.004	0.115± 0.004	0.382± 0.069	0.253± 0.064	0.207± 0.010	0.175± 0.009
7136 [Ar III]	0.096± 0.003	0.074± 0.003	0.049± 0.040	0.032± 0.035	0.055± 0.006	0.045± 0.005
7320 [O II]	0.035± 0.002	0.026± 0.002	0.008± 0.035	0.005± 0.030	0.040± 0.007	0.033± 0.006
7330 [O II]	0.028± 0.002	0.021± 0.002	0.054± 0.036	0.035± 0.031	0.036± 0.007	0.029± 0.006
C(H $\beta$ ), dex	0.27±0.03	...	0.14±0.15	...	0.15±0.03	...
EW(abs), $\text{\AA}$	0.30±0.53	...	2.75±0.36	...	1.30±0.35	...
F(H $\beta$ )	118.8±1.8	...	2.98±0.35	...	34.8±0.7	...
EW(H $\beta$ ), $\text{\AA}$	82± 1	...	8± 1	...	32± 1	...
Rad. vel., km s <sup>-1</sup>	879± 6	...	745±6	...	434± 6	...

**Table 11. Table B.9** Observed and corrected relative fluxes in the lines of void galaxies (SDSS)

$\lambda_0(\text{\AA})$ Ion	UGC4148		NGC2500		MCG7-17-19	
	F( $\lambda$ )/F(H $\beta$ )	I( $\lambda$ )/I(H $\beta$ )	F( $\lambda$ )/F(H $\beta$ )	I( $\lambda$ )/I(H $\beta$ )	F( $\lambda$ )/F(H $\beta$ )	I( $\lambda$ )/I(H $\beta$ )
(3727 [O II])	...	...	0.861±0.087	1.140±0.117	...	...
3868 [Ne III]	...	0.235±0.209	0.145±0.024	0.184±0.030	0.257±0.014	0.274±0.015
4101 H $\delta$	...	...	0.218±0.009	0.267±0.014	0.222±0.011	0.257±0.015
4340 H $\gamma$	0.340±0.119	0.477±0.207	0.430±0.011	0.489±0.014	0.439±0.013	0.471±0.016
4363 [O III]	...	...	...	...	0.044±0.007	0.045±0.008
4861 H $\beta$	1.000±0.182	1.000±0.232	1.000±0.018	1.000±0.019	1.000±0.016	1.000±0.017
4959 [O III]	0.815±0.158	0.777±0.159	0.612±0.013	0.597±0.013	1.070±0.027	1.046±0.027
5007 [O III]	2.304±0.324	2.158±0.365	1.815±0.035	1.753±0.034	3.193±0.080	3.111±0.079
5876 He I	0.093±0.069	0.177±0.130	0.122±0.006	0.100±0.005	0.098±0.005	0.091±0.004
6300 [O I]	...	...	0.041±0.004	0.031±0.003	0.038±0.005	0.034±0.005
6312 [S III]	...	...	0.036±0.004	0.027±0.003	0.014±0.004	0.013±0.004
6548 [N II]	0.063±0.055	0.035±0.045	0.168±0.004	0.123±0.003	0.037±0.005	0.033±0.004
6563 H $\alpha$	3.449±0.487	2.792±0.490	3.751±0.065	2.755±0.052	3.157±0.074	2.821±0.073
6584 [N II]	0.189±0.168	0.106±0.053	0.504±0.010	0.369±0.008	0.110±0.007	0.098±0.006
6717 [S II]	0.503±0.205	0.367±0.090	0.426±0.008	0.306±0.006	0.251±0.008	0.222±0.008
6731 [S II]	0.341±0.200	0.258±0.077	0.305±0.006	0.219±0.005	0.184±0.007	0.163±0.006
7136 [Ar III]	...	0.030±0.035	0.105±0.003	0.071±0.002	0.081±0.005	0.071±0.005
7320 [O II]	0.223±0.276	0.152±0.091	0.030±0.003	0.020±0.002	0.038±0.005	0.033±0.005
7330 [O II]	0.085±0.176	...	0.021±0.003	0.014±0.002	0.032±0.005	0.028±0.005
C(H $\beta$ ), dex	0.20±0.18		0.40±0.02		0.13±0.03	
EW(abs), $\text{\AA}$	0.90±1.08		0.30±0.41		1.50±0.47	
F(H $\beta$ )	4.04±0.46		147.4±1.9		79.7±0.9	
EW(H $\beta$ ), $\text{\AA}$	10.2±1.3		89±1		94±1	
Rad. vel., km s $^{-1}$	709±3		479±3		682±3	

**Table 12. Table B.10** Observed and corrected relative fluxes in the lines of void galaxies (SDSS)

$\lambda_0(\text{\AA})$ Ion	J0810+1837		J0812+4836		NGC2537	
	F( $\lambda$ )/F(H $\beta$ )	I( $\lambda$ )/I(H $\beta$ )	F( $\lambda$ )/F(H $\beta$ )	I( $\lambda$ )/I(H $\beta$ )	F( $\lambda$ )/F(H $\beta$ )	I( $\lambda$ )/I(H $\beta$ )
(3727 [O II])	4.040±2.070	3.652±2.174	...	...	...	...
3868 [Ne III]	...	...	0.417±0.155	0.346±0.155	0.129±0.045	0.126±0.053
4101 H $\delta$	0.075±0.067	0.269±0.343	0.080±0.044	0.294±0.260	0.070±0.024	0.285±0.154
4340 H $\gamma$	0.376±0.073	0.478±0.122	0.266±0.046	0.427±0.118	0.286±0.026	0.462±0.062
4363 [O III]	...	...	...	...	0.066±0.020	0.059±0.022
4740 [Ar IV]	...	...	0.061±0.025	0.051±0.025	...	...
4861 H $\beta$	1.000±0.104	1.000±0.129	1.000±0.079	1.000±0.110	1.000±0.042	1.000±0.057
4959 [O III]	0.843±0.097	0.725±0.096	0.331±0.041	0.274±0.041	0.682±0.026	0.550±0.026
5007 [O III]	2.084±0.171	1.790±0.170	0.994±0.075	0.824±0.075	1.898±0.064	1.520±0.062
5876 He I	0.076±0.049	0.063±0.048	0.053±0.029	0.044±0.029	0.148±0.016	0.105±0.014
6548 [N II]	...	...	0.028±0.018	0.024±0.018	0.228±0.012	0.149±0.010
6563 H $\alpha$	3.283±0.254	2.790±0.273	3.139±0.188	2.712±0.216	3.970±0.128	2.724±0.117
6584 [N II]	0.182±0.077	0.149±0.074	0.084±0.021	0.070±0.021	0.682±0.025	0.446±0.021
6717 [S II]	0.369±0.063	0.203±0.061	0.235±0.024	0.195±0.024	0.486±0.020	0.314±0.017
6731 [S II]	0.235±0.059	0.192±0.056	0.166±0.021	0.138±0.022	0.362±0.017	0.233±0.014
7136 [Ar III]	...	...	0.051±0.015	0.042±0.015	0.121±0.011	0.075±0.009
7320 [O II]	0.060±0.051	0.048±0.048	...	...	0.036±0.010	0.022±0.007
7330 [O II]	0.101±0.052	0.081±0.049	...	...	0.025±0.011	0.015±0.008
C(H $\beta$ ), dex	0.07±0.10		0.00±0.08		0.29±0.04	
EW(abs), $\text{\AA}$	2.25±0.63		2.65±0.70		3.15±0.32	
F(H $\beta$ )	4.04±0.33		7.43±0.41		151.0±4.5	
EW(H $\beta$ ), $\text{\AA}$	14±1		13±1		14±0	
Rad. vel., km s $^{-1}$	1500±9		509±9		440±3	

**Table 13. Table B.11** Observed and corrected relative fluxes in the lines of void galaxies (SDSS)

	NGC2541		J0843+4025		J0911+3135	
$\lambda_0(\text{\AA})$ Ion	F( $\lambda$ )/F(H $\beta$ )	I( $\lambda$ )/I(H $\beta$ )	F( $\lambda$ )/F(H $\beta$ )	I( $\lambda$ )/I(H $\beta$ )	F( $\lambda$ )/F(H $\beta$ )	I( $\lambda$ )/I(H $\beta$ )
(3727 [O II])	...	...	2.110± 0.534	1.947± 0.552	2.099± 0.892	2.081± 1.025
3868 [Ne III]	0.516± 0.015	0.656± 0.020	0.257± 0.093	0.236± 0.095	...	...
4101 H $\delta$	0.231± 0.007	0.282± 0.011	0.119± 0.031	0.243± 0.086	...	...
4340 H $\gamma$	0.416± 0.011	0.473± 0.013	0.406± 0.029	0.487± 0.049	0.332± 0.039	0.476± 0.077
4740 [Ar IV]	0.009± 0.002	0.009± 0.002	...	...	...	...
4861 H $\beta$	1.000± 0.016	1.000± 0.017	1.000± 0.044	1.000± 0.055	1.000± 0.065	1.000± 0.081
4959 [O III]	2.461± 0.062	2.400± 0.061	0.746± 0.035	0.665± 0.035	0.625± 0.044	0.536± 0.044
5007 [O III]	6.693± 0.175	6.463± 0.171	2.294± 0.084	2.043± 0.084	1.884± 0.096	1.608± 0.095
5876 He I	0.118± 0.003	0.097± 0.003	0.161± 0.031	0.141± 0.030	0.226± 0.031	0.178± 0.028
6300 [O I]	0.027± 0.002	0.021± 0.002	0.035± 0.016	0.031± 0.016	0.104± 0.046	0.080± 0.041
6312 [S III]	0.020± 0.002	0.015± 0.002	0.021± 0.015	0.018± 0.015	0.061± 0.043	0.046± 0.038
6548 [N II]	0.021± 0.001	0.015± 0.001	0.028± 0.016	0.024± 0.016	0.033± 0.031	0.025± 0.027
6563 H $\alpha$	3.818± 0.089	2.803± 0.072	3.115± 0.106	2.767± 0.116	3.603± 0.176	2.762± 0.170
6584 [N II]	0.062± 0.005	0.045± 0.004	0.089± 0.020	0.077± 0.019	0.105± 0.037	0.079± 0.032
6717 [S II]	0.112± 0.003	0.081± 0.002	0.251± 0.023	0.216± 0.023	0.302± 0.037	0.224± 0.032
6731 [S II]	0.085± 0.003	0.061± 0.002	0.181± 0.021	0.156± 0.020	0.227± 0.035	0.168± 0.031
7136 [Ar III]	0.087± 0.003	0.059± 0.002	0.061± 0.018	0.052± 0.017	0.043± 0.031	0.031± 0.026
7320 [O II]	0.021± 0.001	0.014± 0.001	0.070± 0.019	0.060± 0.018	0.054± 0.033	0.039± 0.028
7330 [O II]	0.017± 0.001	0.011± 0.001	0.016± 0.015	0.014± 0.015	0.027± 0.033	0.019± 0.027
C(H $\beta$ ), dex	0.40±0.03		0.04±0.04		0.19±0.06	
EW(abs), $\text{\AA}$	1.40±1.09		2.30±0.47		1.80±0.33	
F(H $\beta$ )	214.23±2.45		12.38±0.39		7.39±0.34	
EW(H $\beta$ ), $\text{\AA}$	378± 4		19± 1		12± 1	
Rad. vel., km s $^{-1}$	530± 3		608± 3		742± 3	

**Table 14. Table B.12** Observed and corrected relative fluxes in the lines of void galaxies (SDSS)

	J0928+2845		J0931+2717		J0940+4459	
$\lambda_0(\text{\AA})$ Ion	F( $\lambda$ )/F(H $\beta$ )	I( $\lambda$ )/I(H $\beta$ )	F( $\lambda$ )/F(H $\beta$ )	I( $\lambda$ )/I(H $\beta$ )	F( $\lambda$ )/F(H $\beta$ )	I( $\lambda$ )/I(H $\beta$ )
(3727 [O II])	...	...	1.521± 0.364	1.657± 0.490	1.503± 0.353	1.327± 0.370
3868 [Ne III]	1.009± 0.327	0.634± 0.332	...	...	...	...
4340 H $\gamma$	0.108± 0.070	0.450± 0.613	0.270± 0.073	0.469± 0.184	0.259± 0.092	0.357± 0.169
4861 H $\beta$	1.000± 0.172	1.000± 0.292	1.000± 0.133	1.000± 0.173	1.000± 0.252	1.000± 0.295
4959 [O III]	1.206± 0.165	0.753± 0.165	0.494± 0.082	0.400± 0.080	0.674± 0.181	0.595± 0.181
5007 [O III]	3.639± 0.454	2.271± 0.454	2.128± 0.216	1.706± 0.211	2.044± 0.392	1.804± 0.393
5876 He I	0.233± 0.072	0.145± 0.073	0.091± 0.048	0.062± 0.040	...	...
6548 [N II]	0.126± 0.052	0.078± 0.052	0.095± 0.102	0.058± 0.076	0.022± 0.013	0.020± 0.012
6563 H $\alpha$	4.005± 0.493	2.754± 0.591	4.367± 0.422	2.758± 0.353	3.008± 0.544	2.754± 0.615
6584 [N II]	0.353± 0.067	0.219± 0.069	0.277± 0.105	0.169± 0.079	0.066± 0.039	0.058± 0.039
6717 [S II]	0.677± 0.097	0.419± 0.103	0.528± 0.094	0.317± 0.071	0.327± 0.090	0.289± 0.094
6731 [S II]	0.494± 0.076	0.306± 0.081	0.442± 0.090	0.265± 0.068	0.215± 0.083	0.190± 0.085
7136 [Ar III]	0.083± 0.049	0.051± 0.048	0.106± 0.087	0.060± 0.060	...	...
7320 [O II]	...	...	0.014± 0.057	0.008± 0.038	0.023± 0.044	0.020± 0.044
7330 [O II]	...	...	0.086± 0.057	0.048± 0.039	0.023± 0.044	0.020± 0.044
C(H $\beta$ ), dex	0.01±0.16		0.39±0.12		0.00±0.23	
EW(abs), $\text{\AA}$	2.20±0.23		1.80±0.49		0.95±0.50	
F(H $\beta$ )	6.74±0.82		2.84±0.27		2.72±0.42	
EW(H $\beta$ ), $\text{\AA}$	4± 0		9± 1		7.2±1.2	
Rad. vel., km s $^{-1}$	1216± 3		1492±12		1360± 6	

**Table 15. Table B.13** Observed and corrected relative fluxes in the lines of void galaxies (SDSS)

$\lambda_0(\text{\AA})$ Ion	KISSB23		J0947+4138		J0951+3842	
	F( $\lambda$ )/F(H $\beta$ )	I( $\lambda$ )/I(H $\beta$ )	F( $\lambda$ )/F(H $\beta$ )	I( $\lambda$ )/I(H $\beta$ )	F( $\lambda$ )/F(H $\beta$ )	I( $\lambda$ )/I(H $\beta$ )
(3727 [O II])	1.682± 0.215	1.651± 0.225	...	...	...	...
3868 [Ne III]	0.191± 0.020	0.187± 0.021	0.452± 0.014	0.497± 0.016	...	...
4101 H $\delta$	0.186± 0.012	0.275± 0.024	0.258± 0.008	0.279± 0.012	0.070± 0.059	0.247± 0.311
4340 H $\gamma$	0.409± 0.013	0.473± 0.019	0.476± 0.011	0.501± 0.014	0.304± 0.081	0.480± 0.176
4363 [O III]	...	...	0.122± 0.007	0.127± 0.008	...	...
4740 [Ar IV]	...	...	0.005± 0.003	0.005± 0.003	...	...
4861 H $\beta$	1.000± 0.024	1.000± 0.026	1.000± 0.017	1.000± 0.018	1.000± 0.094	1.000± 0.122
4959 [O III]	0.759± 0.019	0.712± 0.019	1.915± 0.038	1.896± 0.037	1.585± 0.130	1.332± 0.129
5007 [O III]	2.197± 0.050	2.058± 0.050	5.638± 0.111	5.559± 0.110	5.210± 0.376	4.357± 0.372
5876 He I	0.085± 0.010	0.078± 0.009	0.109± 0.004	0.101± 0.004	0.091± 0.090	0.070± 0.082
6300 [O I]	0.023± 0.006	0.021± 0.006	0.012± 0.002	0.011± 0.002	0.068± 0.041	0.051± 0.036
6312 [S III]	0.018± 0.006	0.016± 0.006	0.022± 0.002	0.020± 0.002	...	...
6548 [N II]	0.023± 0.005	0.021± 0.005	0.007± 0.002	0.007± 0.001	0.030± 0.026	0.022± 0.023
6563 H $\alpha$	3.041± 0.061	2.765± 0.065	3.147± 0.052	2.781± 0.050	3.704± 0.262	2.811± 0.257
6584 [N II]	0.069± 0.007	0.062± 0.007	0.022± 0.003	0.019± 0.003	0.101± 0.031	0.074± 0.027
6717 [S II]	0.180± 0.007	0.162± 0.007	0.086± 0.003	0.075± 0.003	0.237± 0.041	0.173± 0.036
6731 [S II]	0.127± 0.006	0.114± 0.006	0.062± 0.003	0.054± 0.003	0.131± 0.035	0.096± 0.030
7136 [Ar III]	0.052± 0.007	0.046± 0.006	0.069± 0.003	0.059± 0.003	...	...
7320 [O II]	0.036± 0.005	0.032± 0.005	0.015± 0.003	0.013± 0.002	...	...
7330 [O II]	0.026± 0.006	0.023± 0.005	0.010± 0.003	0.008± 0.002	...	...
C(H $\beta$ ), dex	0.06±0.03		0.16±0.02		0.18±0.09	
EW(abs), $\text{\AA}$	2.30±0.28		0.30±1.11		2.70±0.74	
F(H $\beta$ )	56.7±1.0		126.1±1.6		4.91±0.33	
EW(H $\beta$ ), $\text{\AA}$	37± 1		183± 2		15± 1	
Rad. vel., km s $^{-1}$	488± 3		1378± 6		1426± 3	

**Table 16. Table B.14** Observed and corrected relative fluxes in the lines of void galaxies (SDSS)

$\lambda_0(\text{\AA})$ Ion	J1000+3032		J1010+4617	
	F( $\lambda$ )/F(H $\beta$ )	I( $\lambda$ )/I(H $\beta$ )	F( $\lambda$ )/F(H $\beta$ )	I( $\lambda$ )/I(H $\beta$ )
3868 [Ne III]	...	...	0.344± 0.054	0.345± 0.059
4101 H $\delta$	...	...	0.119± 0.026	0.216± 0.062
4340 H $\gamma$	0.265± 0.141	0.471± 0.377	0.430± 0.029	0.499± 0.043
4861 H $\beta$	1.000± 0.166	1.000± 0.235	1.000± 0.037	1.000± 0.044
4959 [O III]	0.476± 0.108	0.379± 0.108	1.075± 0.042	0.994± 0.042
5007 [O III]	1.386± 0.199	1.100± 0.197	3.306± 0.118	3.048± 0.117
5876 He I	...	...	0.118± 0.020	0.103± 0.019
6548 [N II]	...	...	0.033± 0.013	0.028± 0.012
6563 H $\alpha$	3.623± 0.434	2.745± 0.452	3.243± 0.110	2.781± 0.111
6584 [N II]	0.094± 0.048	0.068± 0.043	0.097± 0.014	0.082± 0.013
6717 [S II]	0.323± 0.068	0.231± 0.063	0.244± 0.017	0.205± 0.016
6731 [S II]	0.179± 0.055	0.128± 0.050	0.175± 0.016	0.147± 0.015
7136 [Ar III]	0.062± 0.043	0.044± 0.038	0.062± 0.014	0.051± 0.012
7320 [O II]	...	...	0.043± 0.017	0.035± 0.015
7330 [O II]	...	...	0.058± 0.017	0.047± 0.015
C(H $\beta$ ), dex	0.14±0.15		0.12±0.04	
EW(abs), $\text{\AA}$	1.95±0.84		2.05±0.52	
F(H $\beta$ )	2.40±0.28		24.01±0.63	
EW(H $\beta$ ), $\text{\AA}$	8± 1		28± 1	
Rad. vel., km s $^{-1}$	476± 6		1081± 3	

**Table 17. Table B.15** Oxygen abundances in the studied void galaxies (BTA)

Value	UGC3475	UGC3476a	UGC3501	UGC3600	UGC3672	UGC3698a
$T_e(\text{OIII})(\text{K})$	14,533±1082	15,773±1240	17,155±1051	16,404±1037	14,812±1950	16,319±1261
$T_e(\text{OII})(\text{K})$	13,654±1243	14,261±1341	14,716±1082	14,498±1094	13,807±2208	14,469±1335
$\text{O}^+/\text{H}^+(\times 10^5)$	5.514±1.739	1.675±0.513	2.278±0.554	1.677±0.420	3.364±1.785	3.224±0.956
$\text{O}^{++}/\text{H}^+(\times 10^5)$	2.414±0.471	3.462±0.665	1.385±0.201	2.387±0.362	4.569±1.540	2.240±0.414
$\text{O}/\text{H}(\times 10^5)$	7.928±1.802	5.137±0.840	3.664±0.590	4.064±0.554	7.933±2.358	5.464±1.041
$12+\log(\text{O}/\text{H})$	7.90±0.10	7.71±0.07	7.56±0.07	7.61±0.06	7.90±0.13	7.74±0.08
$12+\log(\text{O}/\text{H})(\text{PVT10})$	8.23±0.14	7.76±0.13	7.69±0.17	7.86±0.13	7.94±0.15	8.05±0.11
$12+\log(\text{O}/\text{H})(\text{PM10})$	8.23±0.09	7.74±0.12	7.55±0.13	7.90±0.10	7.98±0.12	7.95±0.09
Value	UGC3698b	NGC2337a	UGC3817	UGC3860	UGC3876	UGC4117
$T_e(\text{OIII})(\text{K})$	14,847±1103	10,475±504	14,173±2021	15,809±1018	15,442±1025	15,018±1175
$T_e(\text{OII})(\text{K})$	13,826±1246	10,441±504	13,443±2366	14,276±1100	14,118±1125	13,914±1317
$\text{O}^+/\text{H}^+(\times 10^5)$	4.627±1.429	4.700±0.834	3.133±1.885	1.215±0.309	2.862±0.753	3.991±1.316
$\text{O}^{++}/\text{H}^+(\times 10^5)$	2.442±0.479	19.190±3.110	4.769±1.793	4.917±0.777	2.773±0.459	2.598±0.549
$\text{O}/\text{H}(\times 10^5)$	7.069±1.507	23.890±3.220	9.214±2.688	6.133±0.836	5.636±0.882	6.589±1.426
$12+\log(\text{O}/\text{H})$	7.85±0.09	8.38±0.06	7.96±0.13	7.79±0.06	7.75±0.07	7.82±0.09
$12+\log(\text{O}/\text{H})(\text{PVT10})$	...	7.93±0.11	8.02±0.15	7.78±0.16	8.25±0.11	7.89±0.26
$12+\log(\text{O}/\text{H})(\text{PM10})$	7.88±0.11	8.06±0.11	8.01±0.11	7.82±0.18	8.26±0.08	7.69±0.16
Value	MCG7-17-19	KUG0821+32	J0843+4025	UGC4704	UGC5272B	UGC5272
$T_e(\text{OIII})(\text{K})$	15,559±1969	16,807±1442	17,994±1060	14,102±1079	14,943±2058	14,656±778
$T_e(\text{OII})(\text{K})$	14,170±2151	14,624±1500	14,879±1071	13,400±1268	13,876±2315	13,723±888
$\text{O}^+/\text{H}^+(\times 10^5)$	3.082±1.520	3.444±1.244	1.487±0.345	2.951±0.983	1.794±0.995	1.879±0.339
$\text{O}^{++}/\text{H}^+(\times 10^5)$	4.130±1.290	0.874±0.217	1.297±0.178	5.288±1.094	2.847±0.995	5.617±0.775
$\text{O}/\text{H}(\times 10^5)$	7.213±1.994	4.318±1.263	2.784±0.389	8.238±1.471	4.641±1.407	7.497±0.845
$12+\log(\text{O}/\text{H})$	7.86±0.12	7.64±0.13	7.44±0.06	7.92±0.08	7.67±0.13	7.87±0.05
$12+\log(\text{O}/\text{H})(\text{PVT10})$	...	...	7.61±0.20	...	7.66±0.23	7.73±0.11
$12+\log(\text{O}/\text{H})(\text{PM10})$	...	7.49±0.24	7.49±0.18	...	7.65±0.26	7.78±0.12

**Table 18. Table B.16** Oxygen abundances in the studied void galaxies (BTA)

Value	J1000+3032	UGCC5427	UGC5464
$T_e(\text{OIII})(\text{K})$	18,389±1521	12,429±1005	12,399±2554
$T_e(\text{OII})(\text{K})$	14,926±1528	12,196±1300	12,171±3312
$\text{O}^+/\text{H}^+(\times 10^5)$	1.807±0.698	4.005±1.568	4.233±4.230
$\text{O}^{++}/\text{H}^+(\times 10^5)$	0.919±0.201	5.813±1.374	4.097±2.461
$\text{O}/\text{H}(\times 10^5)$	2.726±0.726	9.818±2.085	8.330±4.894
$12+\log(\text{O}/\text{H})$	7.44±0.12	7.99±0.09	7.92±0.26
$12+\log(\text{O}/\text{H})(\text{PVT10})$	...	7.91±0.11	8.23±0.11
$12+\log(\text{O}/\text{H})(\text{PM10})$	7.58±0.24	7.92±0.10	8.24±0.08

**Table 19.****Table B.17** Oxygen abundances in the studied galaxies (SDSS)

Value	J1000+3032	J1010+4617
$T_e(\text{OIII})(\text{K})$	19,565±3124	16,098±2701
$T_e(\text{OII})(\text{K})$	15,569±3145	14,389±1010
$\text{O}^+/\text{H}^+(\times 10^5)$	...	2.821±1.160
$\text{O}^{++}/\text{H}^+(\times 10^5)$	0.663±0.243	2.802±1.127
$\text{O}/\text{H}(\times 10^5)$	>0.663±0.243	5.623±1.617
$12+\log(\text{O}/\text{H})$	>6.82±0.16	7.75±0.12
$12+\log(\text{O}/\text{H})(\text{PM10})$	7.34±0.19	7.81±0.09

**Table 20. Table B.18** Oxygen abundances in the studied void galaxies (SDSS)

Value	J0730+4109	J0744+2508	MCG9-13-56	UGC 4148	NGC 2500	MCG 7-17-19
$T_e(\text{OIII})(\text{K})$	12,712±664	22,040±3809	16,538±1081	16,343±2697	14,370±2348	13,280±924
$T_e(\text{OII})(\text{K})$	12,424±522	16,211±3900	14,542±1136	14,477±2852	13,561±2720	12,851±663
$\text{O}^+/\text{H}^+(\times 10^5)$	3.254±0.725	0.721±0.686	2.031±0.454	7.675±11.20	1.758±1.688	3.481±0.976
$\text{O}^{++}/\text{H}^+(\times 10^5)$	7.718±1.164	0.384±0.148	2.009±0.311	1.890±0.775	2.097±0.892	4.725±0.913
$\text{O}^{+++}/\text{H}^+(\times 10^5)$	...	...	...	...	...	0.126±0.055
$\text{O}/\text{H}(\times 10^5)$	10.970±1.371	1.105±0.701	4.039±0.551	9.565±11.22	3.856±1.909	8.333±1.338
$12+\log(\text{O}/\text{H})$	8.04±0.05	7.04±0.28	7.61±0.06	7.98±0.51	7.59±0.21	7.92±0.07
$12+\log(\text{O}/\text{H})(\text{PVT10})$	7.96±0.08	...	7.76±0.14	...	8.35±0.11	...
$12+\log(\text{O}/\text{H})(\text{PM10})$	...	7.28±0.17	7.64±0.08	7.83±0.08	8.38±0.08	7.87±0.08
Value	J0810+1837	J0812+4836	NGC 2537a	NGC 2541	J0843+4025	J0911+3135
$T_e(\text{OIII})(\text{K})$	15,446±2556	22,363±2233	21,521±5311	14,923±281	17,117±1317	17,693±1918
$T_e(\text{OII})(\text{K})$	14,119±2807	16,280±463	16,092±5459	13,866±145	14,707±1358	14,831±1949
$\text{O}^+/\text{H}^+(\times 10^5)$	4.270±2.890	...	0.765±1.086	0.977±0.073	1.994±0.639	1.861±0.970
$\text{O}^{++}/\text{H}^+(\times 10^5)$	1.927±0.800	0.377±0.078	0.766±0.371	7.403±0.383	1.626±0.292	1.195±0.295
$\text{O}^{+++}/\text{H}^+(\times 10^5)$	...	0.025±0.026	...	0.048±0.023	...	0.311±0.352
$\text{O}/\text{H}(\times 10^5)$	6.197±2.999	>0.402±0.082	1.531±1.148	8.428±0.391	3.621±0.703	3.367±1.073
$12+\log(\text{O}/\text{H})$	7.79±0.21	>6.60±0.09	7.18±0.33	7.93±0.02	7.56±0.08	7.53±0.14
$12+\log(\text{O}/\text{H})(\text{PM10})$	7.79±0.14	7.23±0.09	8.40±0.08	7.96±0.08	7.63±0.11	7.54±0.14
Value	J0928+2845	J0931+2717	J0940+4459	KISSB23	J0947+4138	J0951+3842
$T_e(\text{OIII})(\text{K})$	14,973±10346	18,383±1588	18,440±1807	17,423±1076	16,198±501	14,041±1733
$T_e(\text{OII})(\text{K})$	13,891±11620	14,925±1596	14,931±1814	14,778±1100	14,426±533	13,362±1083
$\text{O}^+/\text{H}^+(\times 10^5)$	...	1.557±0.654	1.217±0.548	1.594±0.342	0.702±0.158	...
$\text{O}^{++}/\text{H}^+(\times 10^5)$	2.527±4.422	1.078±0.233	1.221±0.340	1.597±0.225	5.093±0.383	5.562±1.857
$\text{O}^{+++}/\text{H}^+(\times 10^5)$	...	0.402±0.390	...	...	0.123±0.038	0.805±1.227
$\text{O}/\text{H}(\times 10^5)$	>2.527±4.422	3.037±0.797	2.438±0.645	3.192±0.409	5.917±0.416	>6.367±2.226
$12+\log(\text{O}/\text{H})$	> 7.40	7.48±0.11	7.39±0.11	7.50±0.06	7.77±0.03	>7.80±0.15
$12+\log(\text{O}/\text{H})(\text{PVT10})$	...	...	...	7.63±0.14	...	...
$12+\log(\text{O}/\text{H})(\text{PM10})$	7.98±0.11	7.75±0.14	7.49±0.20	7.58±0.09	7.64±0.09	7.92±0.14

**Table 21. Table B.19** Observed and corrected relative fluxes in the lines of galaxies outside the void (BTA)

$\lambda_0(\text{\AA})$ Ion	UGC731		J0839+3140		UGC4787	
	01 10 47.02 +49 36 04.2		08 39 49.05 +31 40 52.4		09 07 35.46 +33 16 42.3	
	F( $\lambda$ )/F(H $\beta$ )	I( $\lambda$ )/I(H $\beta$ )	F( $\lambda$ )/F(H $\beta$ )	I( $\lambda$ )/I(H $\beta$ )	F( $\lambda$ )/F(H $\beta$ )	I( $\lambda$ )/I(H $\beta$ )
3727 [O II]	1.722±0.060	1.627±0.062	1.929±0.766	2.170±0.944	2.346±0.170	2.732±0.206
3868 [Ne III]	0.342±0.023	0.323±0.023	...	...	...	...
3967 [Ne III] + H7	0.205±0.013	0.284±0.022	...	...	0.133±0.015	0.209±0.031
4101 H $\delta$	0.162±0.009	0.239±0.016	...	...	0.227±0.013	0.294±0.023
4340 H $\gamma$	0.442±0.016	0.481±0.019	...	...	0.397±0.017	0.459±0.023
4363 [O III]	0.047±0.009	0.044±0.009	...	...	0.028±0.010	0.029±0.011
4861 H $\beta$	1.000±0.030	1.000±0.032	1.000±0.202	1.000±1.817	1.000±0.031	1.000±0.033
4959 [O III]	1.617±0.047	1.528±0.047	1.214±0.334	1.112±0.331	0.588±0.020	0.566±0.019
5007 [O III]	4.878±0.134	4.609±0.134	3.714±0.572	3.379±0.563	1.829±0.053	1.749±0.053
5876 He I	0.073±0.007	0.069±0.007	...	...	0.089±0.009	0.077±0.008
6300 [O I]	0.028±0.009	0.026±0.009	...	...	0.063±0.010	0.052±0.008
6312 [S III]	0.000±0.002	0.000±0.002	...	...	0.020±0.008	0.016±0.007
6548 [N II]	0.026±0.006	0.024±0.006	...	...	0.067±0.011	0.054±0.009
6563 H $\alpha$	2.733±0.070	2.597±0.076	3.643±0.594	2.799±1.292	3.475±0.090	2.811±0.081
6584 [N II]	0.094±0.021	0.089±0.021	...	...	0.206±0.027	0.166±0.022
6717 [S II]	0.133±0.013	0.125±0.013	...	...	0.402±0.016	0.319±0.014
6731 [S II]	0.115±0.015	0.109±0.015	...	...	0.302±0.015	0.240±0.013
7136 [Ar III]	0.056±0.009	0.052±0.009	...	...	0.056±0.009	0.043±0.007
C(H $\beta$ ), dex	0.00±0.03		0.27±0.21		0.25±0.03	
EW(abs), $\text{\AA}$	5.85±0.38		2.70±63.48		5.70±1.60	
F(H $\beta$ )	4.68±0.09		0.14±0.02		20.6±0.4	
EW(H $\beta$ ), $\text{\AA}$	100±2		35±6		225±5	
Rad. vel., km s <sup>-1</sup>	652±15		406±45		490±42	

**Table 22. Table B.20** Observed and corrected relative fluxes in the lines of galaxies outside the void (BTA)

$\lambda_0(\text{\AA})$ Ion	KUG1004+39		UGC5451a		UGC5451b	
	10 07 22.84 +38 58 20.1		10 07 16.93 +47 00 26.7		10 07 17.90 +47 00 20.0	
	F( $\lambda$ )/F(H $\beta$ )	I( $\lambda$ )/I(H $\beta$ )	F( $\lambda$ )/F(H $\beta$ )	I( $\lambda$ )/I(H $\beta$ )	F( $\lambda$ )/F(H $\beta$ )	I( $\lambda$ )/I(H $\beta$ )
3727 [O II]	1.076±0.031	1.097±0.034	2.943±0.111	2.897±0.125	3.823±0.153	4.048±0.197
3868 [Ne III]	0.445±0.012	0.452±0.013	0.216±0.016	0.211±0.017	0.248±0.028	0.256±0.033
3967 [Ne III] + H7	0.267±0.008	0.295±0.010	0.035±0.005	0.118±0.024	...	...
4101 H $\delta$	0.244±0.009	0.268±0.011	0.209±0.011	0.277±0.017	0.100±0.012	0.231±0.036
4340 H $\gamma$	0.449±0.014	0.468±0.015	0.406±0.018	0.461±0.023	0.392±0.026	0.499±0.040
4363 [O III]	0.087±0.008	0.087±0.009	0.035±0.010	0.033±0.010	0.067±0.019	0.064±0.021
4861 H $\beta$	1.000±0.029	1.000±0.030	1.000±0.043	1.000±0.047	1.000±0.043	1.000±0.050
4959 [O III]	1.762±0.053	1.730±0.053	0.928±0.040	0.863±0.040	0.769±0.037	0.668±0.037
5007 [O III]	5.362±0.142	5.259±0.142	2.763±0.114	2.564±0.113	2.085±0.080	1.799±0.079
5876 He I	0.106±0.004	0.102±0.004	0.103±0.007	0.093±0.006	0.181±0.015	0.140±0.013
6300 [O I]	0.014±0.002	0.013±0.002	0.029±0.004	0.026±0.004	0.090±0.016	0.067±0.013
6312 [S III]	0.030±0.003	0.029±0.003	0.008±0.004	0.007±0.004	0.025±0.013	0.018±0.011
6548 [N II]	0.009±0.002	0.009±0.002	0.076±0.005	0.067±0.005	0.165±0.016	0.120±0.013
6563 H $\alpha$	2.955±0.074	2.808±0.078	3.158±0.108	2.830±0.113	3.681±0.130	2.735±0.119
6584 [N II]	0.028±0.023	0.026±0.023	0.263±0.031	0.231±0.029	0.519±0.045	0.374±0.038
6717 [S II]	0.130±0.005	0.123±0.005	0.381±0.025	0.335±0.024	0.760±0.039	0.541±0.033
6731 [S II]	0.082±0.005	0.077±0.005	0.190±0.022	0.167±0.021	0.527±0.033	0.374±0.028
7136 [Ar III]	0.079±0.003	0.074±0.003	0.057±0.004	0.049±0.004	0.044±0.008	0.030±0.006
C(H $\beta$ ), dex	0.05±0.03		0.07±0.04		0.26±0.05	
EW(abs), $\text{\AA}$	2.95±0.46		2.00±0.18		1.80±0.08	
F(H $\beta$ )	188.7±3.5		12.04±0.35		5.20±0.15	
EW(H $\beta$ ), $\text{\AA}$	188±4		28±1		13±0	
Rad. vel., km s <sup>-1</sup>	544±39		643±12		505±57	



**Table 23. Table B.21** Observed and corrected relative fluxes in the lines of galaxies outside the void (BTA)

$\lambda_0(\text{\AA})$ Ion	J1031+2801		NGC3274a		NGC3274b	
	10 31 55.80	+28 01 33.7	10 32 18.87	+27 39 52.7	10 32 19.71	+27 40 00.9
	F( $\lambda$ )/F(H $\beta$ )	I( $\lambda$ )/I(H $\beta$ )	F( $\lambda$ )/F(H $\beta$ )	I( $\lambda$ )/I(H $\beta$ )	F( $\lambda$ )/F(H $\beta$ )	I( $\lambda$ )/I(H $\beta$ )
3727 [O II]	4.064± 0.732	4.572± 1.073	2.424± 0.064	2.428± 0.073	3.349± 0.088	4.032± 0.116
3868 [Ne III]	...	...	0.339± 0.016	0.337± 0.018	0.218± 0.013	0.255± 0.015
3967 [Ne III] + H7	...	...	0.153± 0.009	0.265± 0.021	...	...
4101 H $\delta$	...	...	0.175± 0.009	0.273± 0.018	0.173± 0.007	0.227± 0.011
4340 H $\gamma$	0.200± 0.042	0.469± 0.150	0.391± 0.014	0.465± 0.020	0.446± 0.013	0.502± 0.016
4363 [O III]	...	...	0.042± 0.010	0.040± 0.010	0.043± 0.007	0.046± 0.007
4861 H $\beta$	1.000± 0.077	1.000± 0.104	1.000± 0.029	1.000± 0.032	1.000± 0.027	1.000± 0.028
4959 [O III]	1.065± 0.085	0.810± 0.083	1.264± 0.036	1.174± 0.035	0.779± 0.022	0.750± 0.022
5007 [O III]	2.888± 0.176	2.166± 0.170	3.755± 0.097	3.477± 0.097	2.395± 0.061	2.286± 0.060
5876 He I	...	...	0.139± 0.010	0.124± 0.009	0.128± 0.006	0.108± 0.005
6300 [O I]	...	...	0.066± 0.007	0.057± 0.006	0.136± 0.007	0.109± 0.006
6312 [S III]	...	...	0.031± 0.007	0.027± 0.007	0.041± 0.008	0.033± 0.007
6548 [N II]	0.053± 0.052	0.028± 0.035	0.044± 0.007	0.038± 0.007	0.067± 0.004	0.052± 0.004
6563 H $\alpha$	5.164± 0.302	2.816± 0.231	3.247± 0.081	2.840± 0.083	3.571± 0.084	2.796± 0.073
6584 [N II]	0.139± 0.057	0.073± 0.038	0.139± 0.027	0.120± 0.025	0.192± 0.026	0.149± 0.021
6717 [S II]	0.405± 0.071	0.207± 0.048	0.356± 0.014	0.306± 0.013	0.545± 0.015	0.418± 0.013
6731 [S II]	0.124± 0.049	0.063± 0.032	0.242± 0.013	0.208± 0.012	0.376± 0.013	0.288± 0.011
7136 [Ar III]	...	...	0.090± 0.010	0.076± 0.009	0.085± 0.006	0.063± 0.005
C(H $\beta$ ), dex	0.52±0.08		0.10±0.03		0.29±0.03	
EW(abs), $\text{\AA}$	1.65±0.15		3.70±0.28		1.65±0.32	
F(H $\beta$ )	7.50±0.40		106.31±1.93		71.58±1.17	
EW(H $\beta$ ), $\text{\AA}$	6± 0.3		52± 1		69± 1	
Rad. vel., km s <sup>-1</sup>	485±75		468±48		441±57	

**Table 24. Table B.22** Observed and corrected relative fluxes in the lines of galaxies outside the void (BTA)

$\lambda_0(\text{\AA})$ Ion	UGC5764a		UGC6055	
	10 36 43.14	+31 32 50.1	10 58 32.40	+48 46 53.4
	F( $\lambda$ )/F(H $\beta$ )	I( $\lambda$ )/I(H $\beta$ )	F( $\lambda$ )/F(H $\beta$ )	I( $\lambda$ )/I(H $\beta$ )
3727 [O II]	0.999± 0.049	1.080± 0.055	2.458± 0.626	2.686± 0.688
3868 [Ne III]	0.402± 0.019	0.430± 0.021	...	...
3967 [Ne III] + H7	0.258± 0.015	0.278± 0.022	...	...
4101 H $\delta$	0.233± 0.014	0.248± 0.021	...	...
4340 H $\gamma$	0.496± 0.020	0.515± 0.025	0.487± 0.043	0.506± 0.057
4363 [O III]	0.082± 0.013	0.085± 0.014	...	...
4861 H $\beta$	1.000± 0.031	1.000± 0.034	1.000± 0.069	1.000± 0.073
4959 [O III]	1.533± 0.041	1.519± 0.041	0.623± 0.048	0.619± 0.048
5007 [O III]	5.724± 0.157	5.655± 0.156	2.034± 0.111	2.015± 0.110
5876 He I	0.122± 0.009	0.115± 0.009	...	...
6300 [O I]	0.023± 0.009	0.021± 0.008	...	...
6312 [S III]	0.028± 0.007	0.026± 0.007	...	...
6548 [N II]	0.019± 0.009	0.017± 0.008	0.037± 0.030	0.034± 0.027
6563 H $\alpha$	3.082± 0.082	2.815± 0.081	3.058± 0.160	2.779± 0.159
6584 [N II]	0.058± 0.026	0.052± 0.024	0.117± 0.042	0.107± 0.038
6717 [S II]	0.123± 0.011	0.112± 0.010	0.366± 0.045	0.330± 0.042
6731 [S II]	0.080± 0.010	0.072± 0.009	0.091± 0.039	0.082± 0.035
7136 [Ar III]	0.081± 0.010	0.072± 0.009	...	...
C(H $\beta$ ), dex	0.12±0.03		0.12±0.07	
EW(abs), $\text{\AA}$	0.55±1.93		0.00±0.76	
F(H $\beta$ )	71.78±1.41		23.75±1.13	
EW(H $\beta$ ), $\text{\AA}$	171± 4		29± 1	
Rad. vel., km s <sup>-1</sup>	523±18		577±171	

**Table 25. Table B.23** Oxygen abundance in the galaxies outside the Lynx-Cancer void (BTA)

Value	UGC731	J0839+3140	UGC4787	KUG1004+392	UGC5451c	UGC5451d
$T_e(\text{OIII})(\text{K})$	11,434±774	14,988±1921	14,159±2169	14,070±602	12,713±1521	20,314±4129
$T_e(\text{OII})(\text{K})$	11,318±1064	13,899±2156	13,434±2541	13,380±708	12,424±1936	14,882±4170
$\text{O}^+/\text{H}^+(\times 10^5)$	4.084±1.516	2.508±1.681	3.943±2.132	1.568±0.240	4.926±2.774	3.761±3.282
$\text{O}^{++}/\text{H}^+(\times 10^5)$	10.820±2.289	3.710±1.315	2.214±0.894	6.796±0.782	4.404±1.514	1.024±0.425
$\text{O}/\text{H}(\times 10^5)$	14.900±2.745	6.218±2.134	6.157±2.312	8.364±0.818	9.330±3.160	4.785±3.309
$12+\log(\text{O}/\text{H})$	8.17±0.08	7.79±0.15	7.79±0.16	7.92±0.04	7.97±0.15	7.68±0.30
$12+\log(\text{O}/\text{H})(\text{PVT10})$	7.88±0.12	...	7.92±0.13	7.76±0.17	8.23±0.12	8.18±0.12
$12+\log(\text{O}/\text{H})(\text{PM10})$	8.00±0.10	...	7.78±0.09	...	8.24±0.08	8.04±0.08
Value	J1031+2801	NGC3274a	NGC3274b	UGC5764a	UGC6055	
$T_e(\text{OIII})(\text{K})$	14,244±1446	12,154±1171	15,316±1129	13,734±925	16,324±1376	
$T_e(\text{OII})(\text{K})$	13,486±1686	11,965±1540	14,059±1248	13,164±1110	14,471±1456	
$\text{O}^+/\text{H}^+(\times 10^5)$	5.841±2.815	4.738±2.273	4.489±1.303	1.499±0.440	2.725±1.117	
$\text{O}^{++}/\text{H}^+(\times 10^5)$	2.802±0.766	6.810±1.947	2.376±0.437	7.440±1.359	1.766±0.361	
$\text{O}/\text{H}(\times 10^5)$	8.643±2.917	11.550±2.993	6.864±1.375	8.939±1.429	4.491±1.174	
$12+\log(\text{O}/\text{H})$	7.94±0.15	8.06±0.11	7.84±0.09	7.95±0.07	7.65±0.11	
$12+\log(\text{O}/\text{H})(\text{PVT10})$	...	7.99±0.11	8.06±0.10	7.85±0.14	...	
$12+\log(\text{O}/\text{H})(\text{PM10})$	...	7.97±0.10	7.86±0.09	7.91±0.15	7.71±0.13	